https://doi.org/10.5194/egusphere-2023-1381
Preprint. Discussion started: 14 August 2023

Temperature-dependent aqueous OH kinetics of C_2-C_{10} linear and terpenoid alcohols and diols: new rate coefficients, structure-activity relationship and atmospheric lifetimes

Bartłomiej Witkowski,[1*] Priyanka Jain,[1] Beata Wileńska,[1] and Tomasz Gierczak[1]

[1]University of Warsaw, Faculty of Chemistry, al. Żwirki i Wigury 101, 02-089 Warsaw, Poland

Correspondence to: Bartłomiej Witkowski (bwitk@chem.uw.edu.pl)

Abstract. Aliphatic alcohols (AAs), including terpenoic alcohols (TAs), are ubiquitous in the atmosphere due to their widespread emissions from natural and man-made sources. Hydroxyl radical (OH) is the most important atmospheric oxidant in both aqueous and gas phases. Consequently, the aqueous oxidation of the TAs by the OH inside clouds and fogs is a potential source of aqueous secondary organic aerosols ($_{aq}$SOAs). However, the kinetic data, necessary to estimate the time scales of such reactions is limited. Here, bimolecular rate coefficients ($k_{OH_{aq}}$) for the aqueous oxidation of twenty-nine, C_2-C_{10} AAs by hydroxyl radicals (OH) were measured with the relative rate method in the temperature range 278 - 328 K. $k_{OH_{aq}}$ values for the fifteen AAs were measured for the first time after validating the experimental approach. The $k_{OH_{aq}}$ values measured for the C_2-C_{10} AAs at 298K were between 1.80×10^9 and 6.5×10^9 $M^{-1}s^{-1}$. The values of activation parameters (activation energy (7-17 kJ/mol) and average Gibbs free energy of activation=20 kJ/mol) strongly indicated the predominance of the H-atom abstraction mechanism.. The estimated rates of the complete diffusion-limited reactions revealed up to 44% diffusion contribution to the measured $k_{OH_{aq}}$ values for the C_8-C_{10} AAs.

The kinetic data acquired here, and the literature data, for AAs, carboxylic acids, and carboxylate ions were used to develop a modified structure-activity relationship (SAR). The new SAR developed in this work predicted the temperature-dependent $k_{OH_{aq}}$ for all compounds under investigation with higher accuracy as compared with the previous models. In the modified model, an additional neighboring parameter was introduced ($F\geq(CH_2)_6$, using the measured $k_{OH_{aq}}$ values for the homolog (C_2-C_{10}) linear alcohols and diols. Good accuracy of the new SAR at 298K (slope=1.05, R^2=0.75) was achieved for the AAs and carboxylic acids under investigation. The kinetic database ($k_{OH_{aq}}$ values in this work and compiled literature data) was also used to further enhance the ability of SAR to predict temperature-dependent values of $k_{OH_{aq}}$ in the temperature range 278 - 328 K.

https://doi.org/10.5194/egusphere-2023-1381
Preprint. Discussion started: 14 August 2023

The calculated atmospheric lifetimes indicate that terpenoic alcohols and diols will react with the OH in aerosol, cloud, and fog water with (LWC≥0.1 g/m^3) and (LWC≥10^{-4} g/m^3), respectively. The preference of terpenoic diols to undergo aqueous oxidation by the OH under realistic atmospheric conditions is comparable with terpenoic acids, which makes them potentially effective precursors of $_{aq}$SOAs. In clouds, a decrease in the temperature will strongly favor the aqueous reaction with the OH, primarily due to the increased partitioning into the aqueous phase following Henry's law equilibrium.

https://doi.org/10.5194/egusphere-2023-1381
Preprint. Discussion started: 14 August 2023

1 Introduction

Biogenic volatile organic compounds (BVOCs) account for 20-90% of the global emissions of non-methane organics into the atmosphere, consisting primarily of isoprene and terpenes, emitted by vegetation (Sindelarova et al., 2022). Moreover, the oxidation of these atmospherically abundant BVOCs in the gas phase is one of the major sources of secondary organic aerosols (SOAs), which are formed following the nucleation of the low-volatility, oxygenated products and their condensation onto the existing particles (Hallquist et al., 2009).

SOAs account for a large fraction of organic aerosol (OA) mass, which contributes up to 90% of fine (submicron) particulate matter (PM) (Jimenez et al., 2009; Xu et al., 2021). SOAs are important climate-forcing agents; they alter the properties of clouds, which affects the Earth's hydrological cycle (Shrivastava et al., 2017; Mahilang et al., 2021). Furthermore, SOAs absorb and scatter solar radiation, thereby affecting the Earth's radiation balance and limiting visibility (Tsigaridis and Kanakidou, 2018). Fine PM inhalation has also been associated with cardiovascular and respiratory conditions, resulting in increased mortality (Pye et al., 2021).

There are still many uncertainties regarding the formation, evolution, and climate forcing of SOAs, which greatly limits the current understanding of the present and future environmental impacts of OAs (Fuzzi et al., 2015; Shrivastava et al., 2017; Mahilang et al., 2021). Historically, gas-phase oxidation of BVOCs was considered the major source of SOA in the atmosphere (Hallquist et al., 2009). More recently, the aqueous and multiphase processing of atmospherically abundant water-soluble organic compounds (WSOCs) emerged as very important atmospheric processes (Su et al., 2020; Carlton et al., 2020). These aqueous and multiphase processes, although still not well characterized, are expected to significantly contribute to the formation of atmospheric SOAs (McNeill, 2015; McVay and Ervens, 2017; Ervens et al., 2018). For instance, the formation of SOAs in the aqueous phase (referred to as $_{aq}$SOAs) can, in part, explain the discrepancies between observed and modeled budgets of OAs (Lin et al., 2014; Tsui et al., 2019; Su et al., 2020; Pai et al., 2020).

Alcohols are one of the major classes of WSOCs in the atmosphere; they are emitted from both natural and man-made sources (Mellouki et al., 2015), and include short and longer-chain (fatty) linear alcohols and diols, as well as cyclic, terpenoic alcohols (TAs) (Guenther et al., 2012; Chen et al., 2021; Konjević et al., 2023). In the atmosphere, hydroxyl radical (OH) is the most important daytime oxidant (Herrmann et al., 2015; Mahilang et al., 2021). Hence, the saturated (aliphatic) WSOCs, such as AAs, are expected to react primarily with OH and NO_3 (Mellouki et al., 2015). In addition to reaction in the gas phase (Ceacero-Vega et al., 2012), AAs can also undergo aqueous oxidation by the OH (RI) inside the aqueous particles, depending on their Henry's law constants (H, M/atm^{-1}) values and liquid water content (LWC, g/m^3) of clouds, fogs, and aerosols (Sander, 2015; Herrmann et al., 2015).

https://doi.org/10.5194/egusphere-2023-1381
Preprint. Discussion started: 14 August 2023

$$AA + OH_{aq} \rightarrow \text{products} \quad \text{(RI)}$$

Consequently, in the atmospheric aqueous droplets, RI can yield low-volatility products, like for instance carboxylic (and terpenoic) acids (Yasmeen et al., 2011; Witkowski et al., 2023). Therefore, TAs (and diols) may be efficient precursors of $_{aq}$SOAs. Due to their large carbon backbones (C_7-C_{10}) and cyclic structures, TAs have the potential to incorporate a relatively large number of oxygenated functional groups without undergoing extensive fragmentation (Ceacero-Vega et al., 2012). However, to date, there have not been many studies that investigated the aqueous OH kinetics of TAs (Hoffmann et al., 2009; Gligorovski et al., 2009; Herrmann et al., 2015; Leviss et al., 2016).

To evaluate whether or not reaction with the OH is a relevant removal pathway for a given molecule under realistic atmospheric conditions, chemical, aqueous and multiphase models are utilized (Bräuer et al., 2019; Zhu et al., 2020). Bimolecular reaction rate coefficients for the reaction of organic compounds with the OH in the gas ($k_{OH_{gas}}$) and in the aqueous ($k_{OH_{aq}}$) phases are the foundation of both simple and complex models (Herrmann et al., 2015), used to investigate the reaction (removal) pathways for various WSOCs (Zhu et al., 2020).

Following decades of research, extensive gas-kinetic databases are available for the reactions of various VOCs with the atmospherically-relevant oxidants (McGillen et al., 2020). On the other hand, the currently available aqueous kinetic datasets are still limited and contain primarily room-temperature data (Buxton et al., 1988; Herrmann et al., 2015). Reliable kinetic datasets are crucial for an accurate parametrization of the complex aqueous and multiphase reactions, which are directly connected with the formation and processing of $_{aq}$SOAs in the atmosphere (Ervens, 2015; Bräuer et al., 2019).

In this work, the values of $k_{OH_{aq}}$ for linear and terpenoic alcohols and diols were measured with the relative rate technique, after validating the experimental approach, to further expand the current solution kinetic databases. Here, $k_{OH_{aq}}$ for multiple AAs were measured in a single experiment; RI was carried out in a bulk reactor and the concentrations of individual AAs in the reaction solution were measured with gas chromatography (Herrmann et al., 2005). Because the temperature range in the atmosphere extends above and below room temperature, the kinetic measurements were carried out in the temperature range between 278 and 328 K.

However, measuring the k_{OH} values for the numerous WSOCs present in the environment is unfeasible (Goldstein and Galbally, 2007). For this reason, structure-activity relationships (SARs) are widely utilized in the field of atmospheric chemistry for estimating the k_{OH} values of various organic molecules based on their molecular structures (Kwok and Atkinson, 1995; Monod and Doussin, 2008). At the same time, the ability of current aqueous SARs to predict the temperature-dependent $k_{OH_{aq}}$ values for the higher-MW WSOCs (with larger carbon

https://doi.org/10.5194/egusphere-2023-1381
Preprint. Discussion started: 14 August 2023

backbones) remains limited (Herrmann et al., 2005; Bräuer et al., 2019). Furthermore, the methodology used in the current aqueous kinetic SARs was developed for predicting the values of $k_{OH_{gas}}$ (Kwok and Atkinson, 1995; Monod and Doussin, 2008).

The kinetic data acquired in this work, and the compiled literature data, were used to develop a modified kinetic SAR for predicting the values of $k_{OH_{aq}}$ for AAs, carboxylic acids, and carboxylate ions at different temperatures. Subsequently, the atmospheric lifetimes for the five TAs under investigation due to RI were estimated to evaluate their potential to yield $_{aq}$SOAs under realistic atmospheric conditions.

2 Materials and methods

Materials and reagents are listed in section S1 in the Electronic Supplementary Material (ESM). Deionized (DI) water (18 MΩ×cm^{-1}) was used in all experiments.

2.1 Aqueous photoreactor

The photoreactor was described in our previous work (Witkowski et al., 2019). The reaction vessel was a jacketed, quartz flask with an internal volume of 0.1 L. Radicals (OH) were generated *in situ* by photolyzing hydrogen peroxide (H_2O_2). The reaction vessel was surrounded by eight lamps (TUV TL 4W, Philips, λ_{max}=254 nm). In some experiments, an ozone-free, 2.12" pen-ray lamp (11SC-2.12-PO-16-800, Analytik Jena, λ_{max}=254 nm) was used. The pen-ray lamp was immersed in the reaction solution inside a quartz vial. Temperatures of the reaction solution were adjusted using a circulating water bath (SC100 a10, Thermo Fisher Scientific). The solution temperature was additionally checked with an externally calibrated platinum sensor (TP-361, Czaki Thermo-Product).

2.2 Chromatographic analyses

Analysis of AAs was carried out with gas chromatography (GC) coupled with the flame ionization detector (FID) or with mass spectrometry (MS).

GC/MS analyses were carried out with a GC/MS-QP2010 Ultra (Shimadzu) gas chromatograph coupled with a single-quadrupole mass spectrometer equipped with an electron ionization (70 eV) ion source. The instrument was equipped with an AOC-5000 autosampler (Shimadzu). Analytes were separated with a VF-WAXms column (Agilent) or with a ZB-5MSplus column (Phenomenex) - section S2.1. The mass spectrometer was operating in the selected ion monitoring mode (Table S1).

https://doi.org/10.5194/egusphere-2023-1381
Preprint. Discussion started: 14 August 2023

GC/FID analyses were carried out using a GC17A gas chromatograph (Shimadzu). Analytes were separated with a ZB-Waxplus capillary column (Phenomenex). This instrument was used for analyzing C_5-C_{10} linear alcohols and diols, as well as for analyzing the C_2-C_5 linear alcohols and diols (section S2.2).

2.3 Experimental procedures

AAs under investigation were separated into four sets, based on their OH reactivities, chromatographic peak shape on a given stationary phase, GC detector response, and recoveries obtained following liquid-liquid extraction of aqueous samples from the photoreactor with ethyl acetate (see below).

The concentration of cyclic, terpenoic, and C_5-C_{10} alcohols (Tables S1 and S2) in the reaction solution was 0.2 - 0.4 mM each, and the concentration of H_2O_2 was 0.1 M. The concentration of C_2-C_5 linear alcohols and diols (Table S2) in the reaction solution was 0.8 – 1.0 mM each, and the concentration of H_2O_2 in these experiments was 0.4 M.

AAs under investigation were first dissolved in water, the resulting solution was filtered through a 0.7 µm GF syringe filter and transferred to the reaction vessel. The temperature of the solution was allowed to stabilize before adding H_2O_2, which initiated the reaction.

Thirteen aliquots were sampled from the reaction solution and the reaction time was 15-70 mins, depending on the temperature and concentration of H_2O_2. The C_2-C_5 AAs (Table S2) were analyzed by injecting 0.5 µl of the aqueous sample taken from the reactor into the GC/FID instrument. For the rest of the AAs under investigation, 800 µl of the reaction solution was saturated with NaCl, and extracted with 300 µl of ethyl acetate containing 0.3 mM of dimethyl phthalate (internal standard). Afterward, the organic layer was dried with anhydrous sodium sulfate (Na_2SO_4) and analyzed with GC/MS or GC/FID instrument.

2.4 Relative rate method and activation parameters

The $k_{OH_{aq}}$ values for the AAs under investigation were derived with eq. I.

$$\mathrm{Ln}\left(\frac{[\mathrm{AA}]_0}{[\mathrm{AA}]_t}\right) = \frac{k_{AA}}{k_{Ref}}\mathrm{Ln}\left(\frac{[\mathrm{Ref}]_0}{[\mathrm{Ref}]_t}\right) \quad \text{(I)}$$

In eq. I, [AA], and [Ref] are the initial (0) and intermediate concentrations of the AAs under investigation and the kinetic reference compound, respectively. k_{Ref} and k_{AA} ($M^{-1}s^{-1}$) are the $k_{OH_{aq}}$ for the kinetic reference compound and the AAs under investigation at a given temperature, respectively. 1,4-Butanediol and 1,5-pentanediol ($k_{OH_{aq}}$ at 298K=$(3.8\pm0.2)\times10^9$ and $(4.4\pm0.7)\times10^9$ $M^{-1}s^{-1}$, respectively) were used as the kinetic reference compounds (Hoffmann et al., 2009).

https://doi.org/10.5194/egusphere-2023-1381
Preprint. Discussion started: 14 August 2023

150 The temperature-dependent $k_{OH_{aq}}$ values were used to obtain the pre-exponential factors (A) and activation energies (E_a) using the Arrhenius expression (eq. II).

$$\mathrm{Ln}(k_{OH_{aq}}) = \mathrm{Ln(A)} - \left(\frac{E_a}{R}\right) \cdot \frac{1}{T} \quad \text{(II)}$$

In eq. II, $k_{OH_{aq}}$ is the bimolecular reaction rate coefficient of the reaction of AAs with the OH (M^{-1} s^{-1}) at a given temperature, T is the temperature (K), R is the gas constant (kJ K^{-1} mol^{-1}), A is the pre-exponential factor (M^{-1} s^{-1}) and E_a is the activation energy (kJ mol^{-1}). The values of Gibbs free energy of activation ($\Delta G^{\ddagger}$), the enthalpy of activation ($\Delta H^{\ddagger}$), and the entropy of activation ($\Delta S^{\ddagger}$) were also calculated for each AA, using the temperature-dependent $k_{OH_{aq}}$ values (section S4). The rates of diffusion-limited reactions (k_{diff}, $M^{-1}s^{-1}$) were derived with the Smoluchowski equation (section S5) (Schöne et al., 2014; Kroflič et al., 2020).

2.5 Structure-activity relationship

The kinetic SAR model used in this work was originally introduced by Atkinson (Atkinson, 1987), and later expanded for estimating the values of $k_{OH_{aq}}$ of aliphatic molecules containing C, H, and O atoms by Monod and Doussin (Monod and Doussin, 2008; Doussin and Monod, 2013). SAR parameters include F and G substituent factors for CH_3, CH_2, CH, C, OH, FC=O, COOH, COO- moieties, F-factors for the C_6, C_5, C_4 rings, and base rate coefficients for the H-atom abstraction from CH_3, CH_2, CH and -OH groups (Fig. 1).

https://doi.org/10.5194/egusphere-2023-1381
Preprint. Discussion started: 14 August 2023

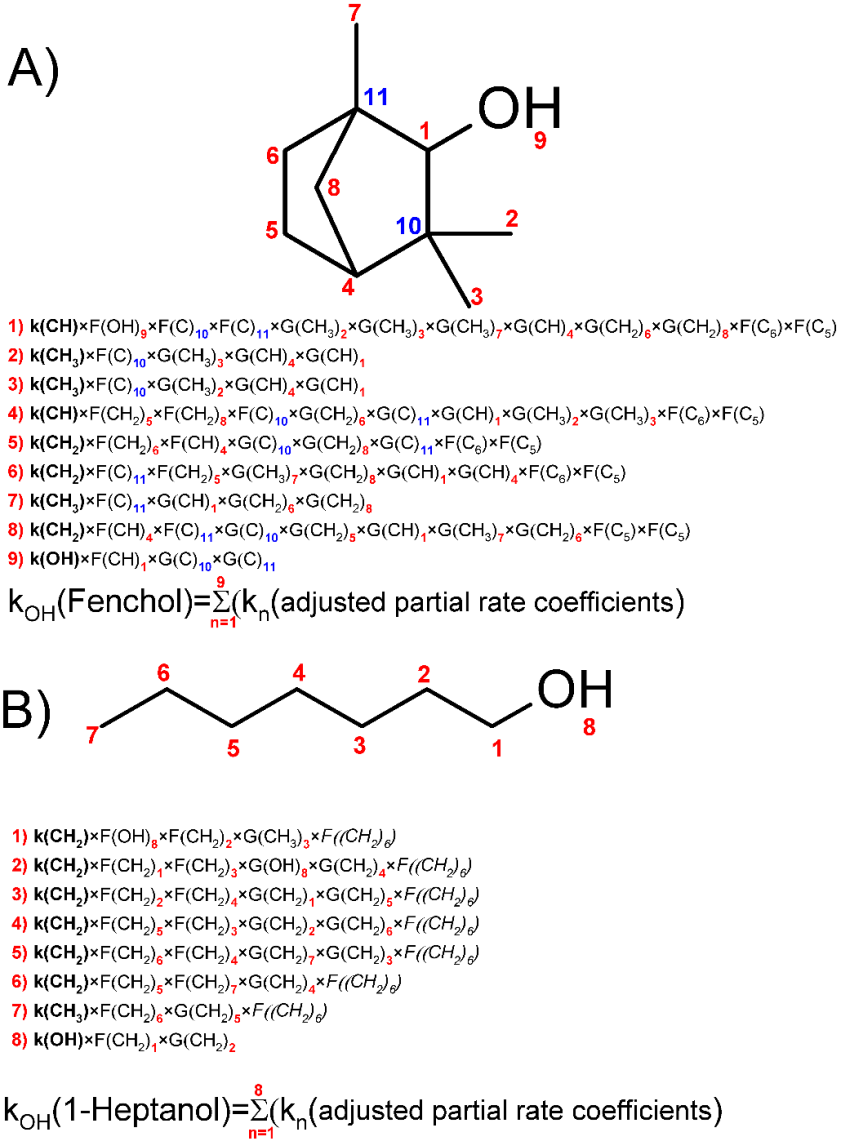

Figure 1: Estimating the values of $k_{OH_{aq}}$ with SAR for fenchol (A) and 1-heptanol (B).

The partial rate coefficients are adjusted by the adjacent functional groups in the α and β-positions using the F and G substituent factors (Monod and Doussin, 2008; Doussin and Monod, 2013). Note that fenchol has two fused C_5 rings and one C_6 ring, and the partial k values for H-atom abstraction connected with these rings are adjusted with

https://doi.org/10.5194/egusphere-2023-1381
Preprint. Discussion started: 14 August 2023

the F(C_5), and F(C_6) factors - Fig. 1A (Monod and Doussin, 2008). Furthermore, in this work, an additional F factor was introduced for the H-atoms connected with a straight-chain carbon backbone≥C_6 (Fig. 1B).

A database containing the values of $k_{OH_{aq}}$ (298 K) for 56 AAs, carboxylic acids, and carboxylate anions (1) was used to derive the values of F and G factors by minimizing values of Q parameter (eq. III) using the Excel Solver routine (González-Sánchez et al., 2021).

$$Q = \sum_n \frac{(k_{SAR} - k_{exp})^2}{\sigma_n^2} \qquad \text{(III)}$$

In eq. III, $k_{SAR,}$ and k_{exp} are estimated and measured $k_{OH_{aq}}$ values at 298K and σ is the experimental uncertainty.

The temperature dependence of the partial k_{OH} values for CH_3, CH_2, CH, and OH groups is described via eq. IV using C and D factors. (Kwok and Atkinson, 1995) C and D factors in eq. IV were adjusted using a database of 351 temperature-dependent rate coefficients (1).

$$k_{OH_{partial}}(T) = CT^2 \times exp\left(\frac{-D}{T}\right) \quad \text{(IV)}$$

In eq. IV, T is the reaction temperature (K). Furthermore, the values of F and G factors were adjusted at different temperatures with eq. V.

$$F \text{ or } G(T) = exp\left(\frac{298 \times ln(F \text{ or } G \text{ at } 298K)}{T}\right) \qquad \text{(V)}$$

After adjusting the values of the neighboring parameter (F and G), they were kept unchanged and the values of D and C factors (eq. IV) were adjusted with the measured, temperature-dependent $k_{OH_{aq}}$ values for AAs (this work) and for carboxylic acids (Witkowski et al., 2021).

2.6 Control measurements and uncertainty

Kinetic measurements at every temperature were carried out a minimum of three times and the experimental uncertainties for the $k_{OH_{aq}}$ were calculated as 2σ. Uncertainties of the activation parameters derived from linear regression analysis are reported as standard errors of the linear fitting. Other uncertainties were calculated with the exact differential method.

Control experiments carried out without turning on the lamp or without adding H_2O_2 to the reaction solution, confirmed that the AAs under investigation did not undergo direct photolysis or dark reactions with the H_2O_2, within the time scale of the experiments. To confirm that the five terpenoic alcohols and diols under investigation were photochemically stable under the experimental conditions used, their UV-Vis spectra were acquired (Fig. S5). Also, no evaporation of the analytes was observed within the studied temperature range (section 2.1). Control

https://doi.org/10.5194/egusphere-2023-1381
Preprint. Discussion started: 14 August 2023

experiments also confirmed that the AAs that were analyzed in the same batch (section S3) were not converted into one another following RI.

3 Results and discussion

3.1 Results of the kinetic measurements

The rate coefficients were calculated using eq. I (section 2.4). In all kinetic measurements the squared linear coefficients of determination (R^2)>0.99 were obtained, as shown in the representative relative kinetic plots (Fig. 2).

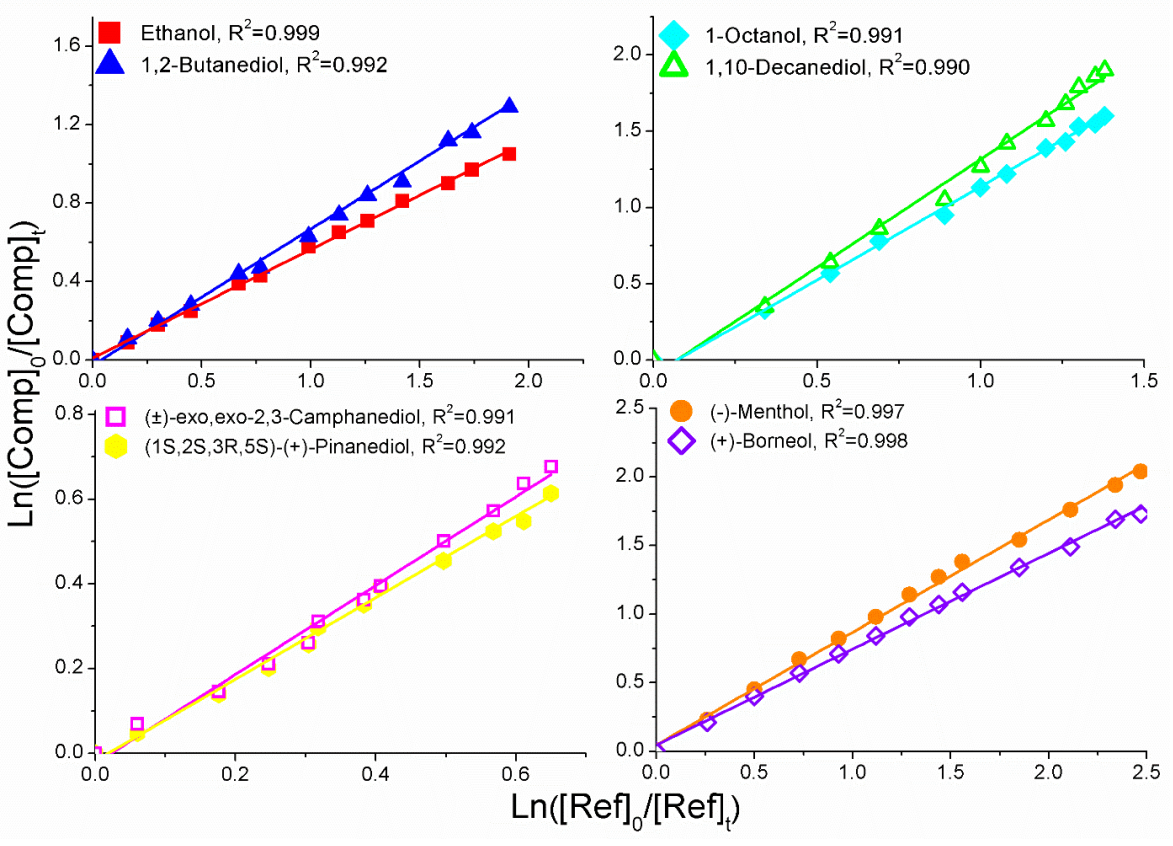

Figure 2: Sample relative kinetic plots obtained at 298K; data are represented by points, and lines are linear fits to the experimental data.

https://doi.org/10.5194/egusphere-2023-1381
Preprint. Discussion started: 14 August 2023

The measured, temperature-dependent values of $k_{OH_{aq}}$ were used to obtain activation parameters (eq. II). For all AAs under investigation, linear plots were obtained, as shown in the sample Arrhenius plots (Fig. 3).

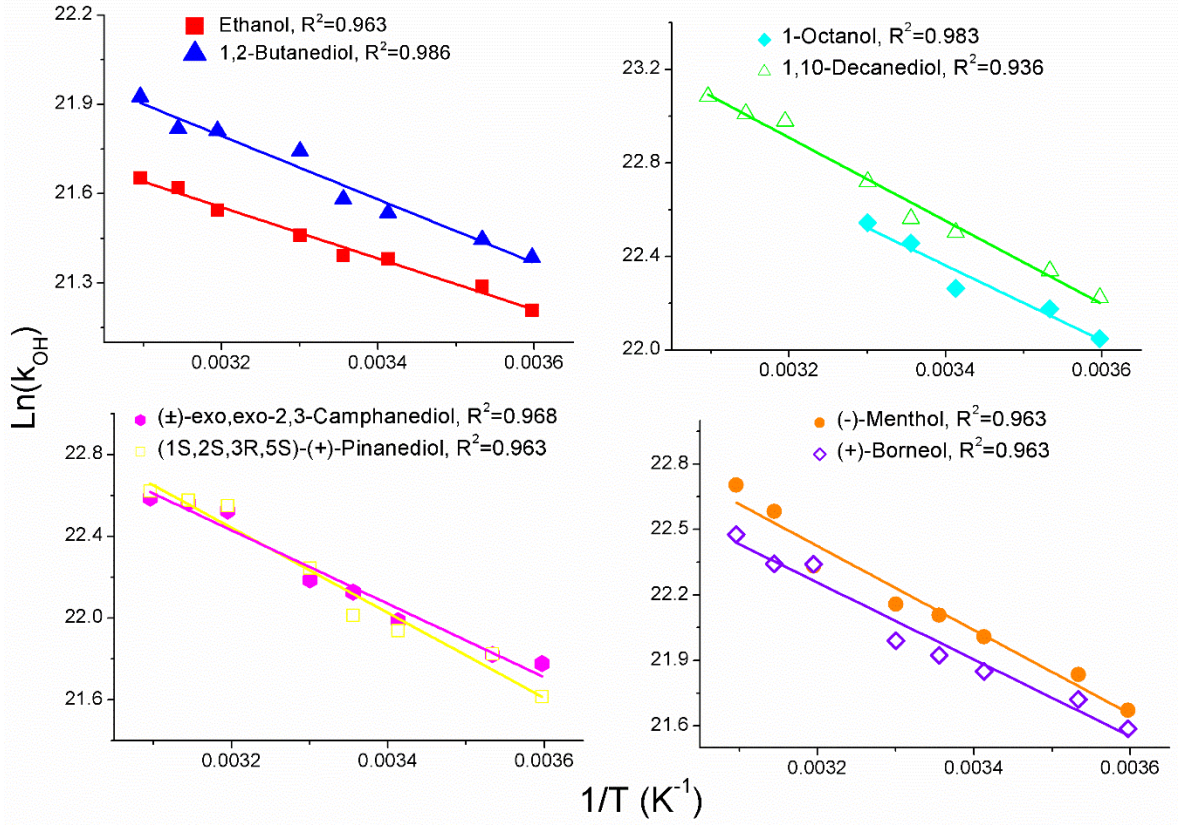

Figure 3: Sample Arrhenius plots obtained; data are represented by points, and lines are linear fits to the experimental data.

The $k_{OH_{aq}}$ values measured at 298 K and the activation parameters for the AAs investigated in this work are listed in Table 1; literature data for the kinetic reference compounds are also included. All temperature-dependent $k_{OH_{aq}}$ values measured in this work are listed in Table S4.

https://doi.org/10.5194/egusphere-2023-1381
Preprint. Discussion started: 14 August 2023

Table 1. The values of $k_{OH_{aq}}$ obtained in this work for the reaction of OH with AAs at 298K and comparison with literature values

Compound	k_{OH} at 298 K, $(M^{-1}s^{-1})\times10^{-9}$		Ref.
	This work	Literature	
Ethanol	1.95±0.07	2.1±0.1	(Ervens et al., 2003)
		1.9[a]	(Buxton et al., 1988)
		1.9	(Park and Getoff, 1992)
1-Propanol	2.48±0.09	3.2±0.2	(Ervens et al., 2003)
		2.5±0.6	(Scholes and Willson, 1967)
		2.8[a]	(Buxton et al., 1988)
		2.7±0.7	(Herrmann et al., 2005)
2-Butanol	2.45±0.11	3.5±0.4	(Herrmann, 2003)
		3.1	(Buxton et al., 1988)
1-Butanol	3.21±0.13	3.7±1	(Scholes and Willson, 1967)
		4.2[a]	(Buxton et al., 1988)
		4.1±0.8	(Herrmann, 2003)
		4.0	(Reuvers et al., 1973)
1-Pentanol	4.50±0.06	4.1±1	(Scholes and Willson, 1967)
		3.8	(Reuvers et al., 1973)
1-Hexanol	4.89±0.05	4.7±1	(Scholes and Willson, 1967)
		7.0	(Buxton et al., 1988)
1-Heptanol	4.98±0.06	4.9±1	(Scholes and Willson, 1967)
		7.4	(Buxton et al., 1988)
1-Octanol	5.66±0.09	5.2±1	(Scholes and Willson, 1967)
		7.7	(Buxton et al., 1988)
1-Nonanol	5.42±0.08		
1-Decanol	6.25±0.03		
3-ethyl-3-pentanol	2.52±0.11		
1,2-Ethanediol	1.86±0.04	1.7±0.03	(Hoffmann et al., 2009)
		2.4	(Matheson et al., 1973)
		1.4	(Adams et al., 1965)
		1.4±0.3	(Scholes and Willson, 1967)
		1.4[a]	(Buxton et al., 1988)

https://doi.org/10.5194/egusphere-2023-1381
Preprint. Discussion started: 14 August 2023

1,2-Propanediol	1.80±0.07	1.7±0.3	(Hoffmann et al., 2009)
		1.7	(Adams et al., 1965)
		1.5±4	(Scholes and Willson, 1967)
		1.7	
1,2-Butanediol	2.36±0.06	2.3±0.4	(Hoffmann et al., 2009)
1,6-Hexanediol	4.93±0.14	4.7	(Anbar et al., 1966)
1,7-Heptanediol	5.43±0.04		
1,8-Octanediol	5.51±0.08		
1,9-Nonanediol	6.37±0.05		
1,10-Decanediol	6.29±.0.06		
Cyclohexanol	3.61±0.09		
trans-1,2-Cyclohexanediol	2.89±0.05		
exo-Norborneol	1.89±0.06		
cis-2-Methylcyclohexanol	4.78±0.52		
(+)-Fenchol	2.99±0.05		
(+)-Borneol	3.32±0.11		
(−)-Menthol	3.99±0.09		
(±)-*exo*,*exo*-2,3-Camphanediol	4.07±0.07		
(1S,2S,3R,5S)-(+)-Pinanediol	3.63±0.12		

[a]For clarity, the average value compiled in the cited references is listed

The majority of the $k_{OH_{aq}}$ values measured in this work at 298K are generally in very good agreement with the literature data, thereby confirming that the experimental approach used in this work is reliable (Table 1). At the same time, lower values of $k_{OH_{aq}}$ for 1 and 2-butanol were reported (Table 1); unfortunately, these discrepancies are somewhat difficult to explain Nevertheless, the values of $k_{OH_{aq}}$ = (4.1±0.8)×10^9 and (3.7±1)×10^9, reported for 1 and 2-butanol, respectively, agree (within the reported uncertainties) with the results obtained in this work (Table 1) (Scholes and Willson, 1967; Herrmann, 2003).

An increase in the measured $k_{OH_{aq}}$ values is observed for the n-alcohols and α,ω-diols (Fig. 4).

https://doi.org/10.5194/egusphere-2023-1381
Preprint. Discussion started: 14 August 2023

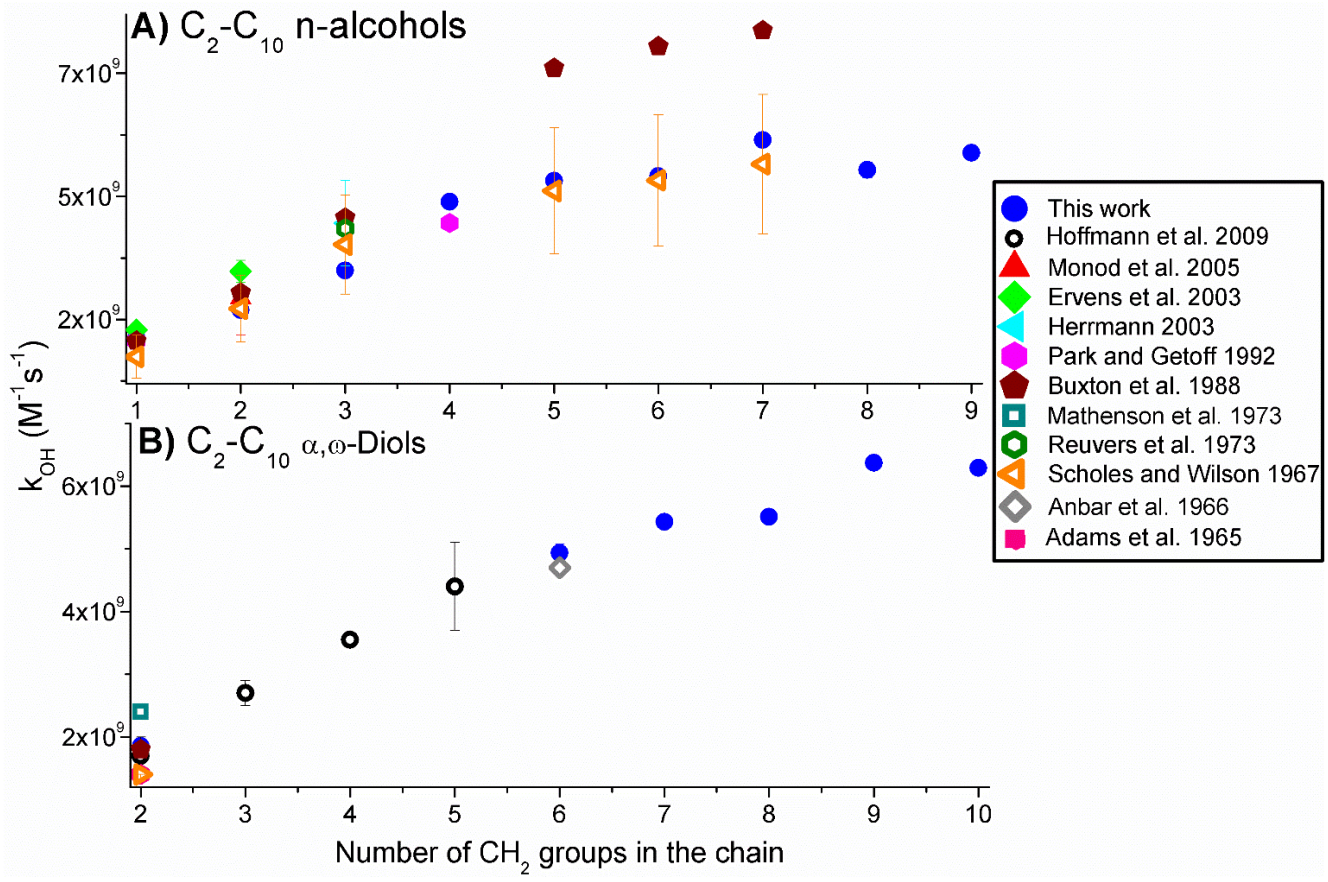

Figure 4: The $k_{OH_{aq}}$ values measured at 298K for the homolog series of linear alcohols (A) and diols (B).

There is some ambiguity regarding the values of $k_{OH_{aq}}$ of C_6-C_8 n-alcohols: Scholes and Wilson report lower values (Table 1) (Scholes and Willson, 1967). However, the values adjusted using a higher $k_{OH_{aq}}$ for thymine, which was the kinetic reference compound used in their study (Scholes and Willson, 1967), are cited most often (Monod and Doussin, 2008; Minakata et al., 2009; Luo et al., 2017). At the same time, following the general trend in Fig. 4A, the $k_{OH_{aq}}$ values of 7.0, 7.4, and 7.7 (Table 1) for C_6-C_8 n-alcohols, respectively, can be tentatively classified as outliers.

The characteristic curving of the plots in Fig. 4A (and to a lesser extent in Fig. 4B) is most likely because of the short-range activating effect of -OH groups, which does not extend beyond three to four -CH_2- moieties (Mellouki et al., 2003; Herrmann et al., 2005). Moreover, a net increase in the values of $k_{OH_{gas}}$ for n-alcohols as compared with n-alkanes is observed (Fig. 5A), likely due to the formation of a hydrogen-bonded complex between -OH moiety and OH radical (Smith and Ravishankara, 2002; Mellouki et al., 2003; Herrmann et al., 2005).

https://doi.org/10.5194/egusphere-2023-1381
Preprint. Discussion started: 14 August 2023

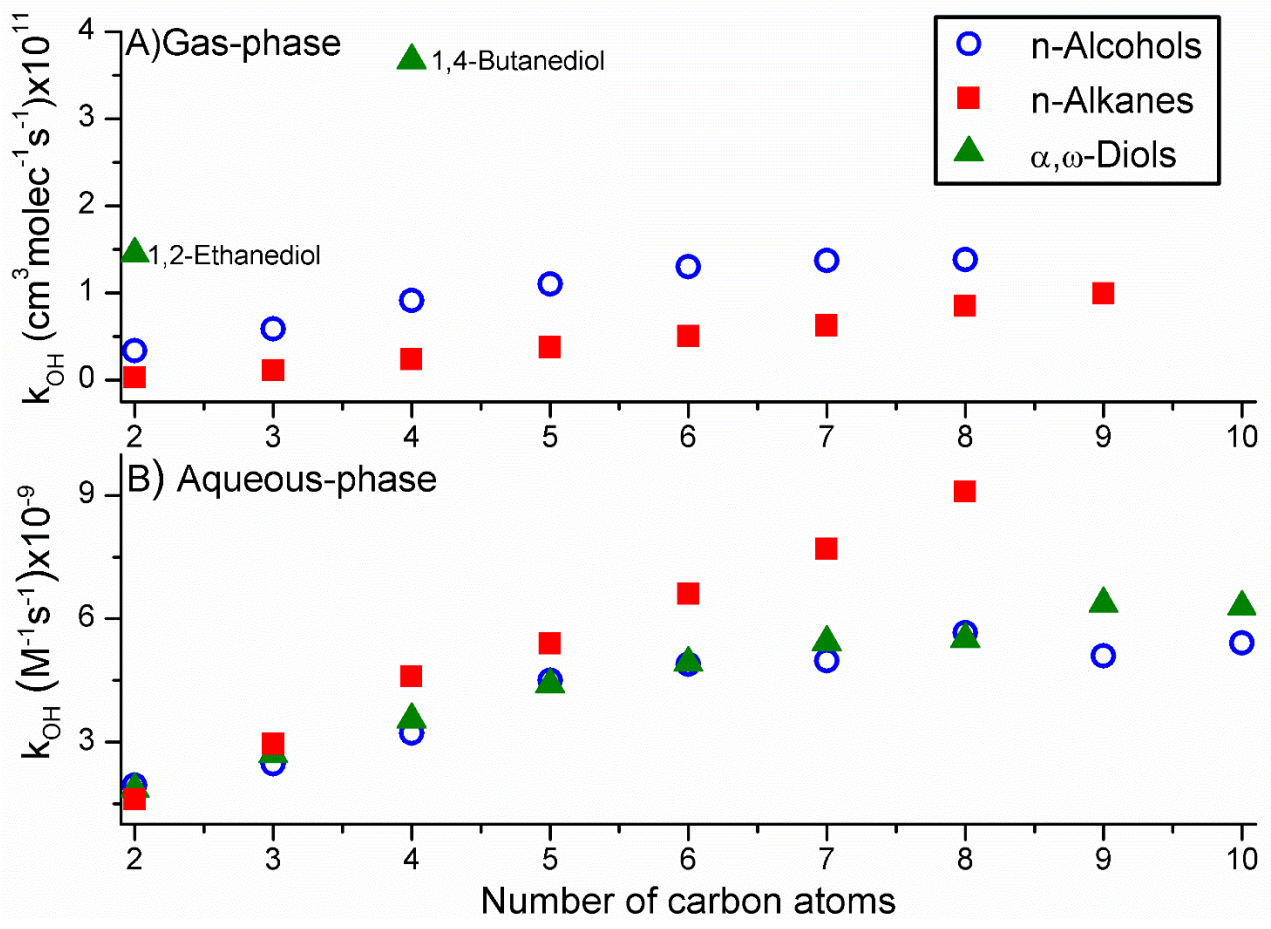

Figure 5: Measured k_{OH} values for n-alkanes, alcohols, and diols in the gas (A) and aqueous (B) phases. The $k_{OH_{gas}}$ values presented are listed in Table S5.

No net increase in the values of $k_{OH_{aq}}$ is observed following the addition of one or two -OH moieties to the carbon backbone (Fig 5B), which can be attributed to solvent effects suppressing the formation of the H-bonded complex between OH and n-alcohols, and α,ω-diols. Solvents effects, such as hydrophobic interactions may also contribute to this phenomenon, such as the formation of hydration spheres around the hydrophobic alkyl chain (Otto and Engberts, 2003). Consequently, in the aqueous solutions, RI likely proceeds via direct H-atom abstraction from the aliphatic chain, as in the case of alkanes (Herrmann et al., 2005), which results in the observed decrease of the $k_{OH_{aq}}$ of n-alcohols and α,ω-diols, as compared with n-alkanes (Fig. 5B).

The values of E_a obtained in this work are much higher (7-15 kJ × mol^{-1} - Table 2) than the values for the same reactions in the gas phase, which also indicates a different, higher-energy transition state in the aqueous phase (Mellouki et al., 2003).

https://doi.org/10.5194/egusphere-2023-1381
Preprint. Discussion started: 14 August 2023

Table 2. The values of activation parameters obtained in this work for the reaction of OH with AAs

Compound	A $\times 10^{-11}$ ($M^{-1}s^{-1}$)	E_A (kJ/mol)	$\Delta H^{\ddagger}$ (kJ/mol)	$\Delta S^{\ddagger}$ (J/mol×K)	$\Delta G^{\ddagger}$ (kJ/mol)	$R^{2,a}$
Ethanol	0.4±0.05	7.1±0.3	4.6±0.3	-(51.2±1.1)	19.9±0.5	0.984
1-Propanol	0.8±0.1	8.5±0.4	6.0±0.4	-(44.7±1.2)	19.3±0.5	0.989
2-Butanol	1.9±0.3	10.6±0.3	8.1±0.3	-(37.5±1.1)	19.3±0.5	0.994
1-Butanol	2.5±0.3	10.7±0.3	8.3±0.3	-(34.9±0.9)	18.7±0.4	0.995
1-Pentanol	6.2±1.3	12.1±0.5	9.7±0.5	-(27.4±1.8)	17.8±0.7	0.989
1-Hexanol	8.2±2.6	12.6±0.8	10.1±0.8	-(25.2±2.6)	17.6±1.1	0.978
1-Heptanol	14.4±6.1	13.9±1.1	11.4±1.1	-(20.5±3.5)	17.5±1.5	0.966
1-Octanol	26.6±1.3	14.1±2.0	11.6±2	-(19.4±6.8)	17.4±2.8	0.944
1-Nonanol	26.6±2.1	15.1±1.2	12.6±3.2	-(15.4±7.2)	17.2±1.6	0.968
1-Decanol	32.8±2.6	15.6±2.6	13.1±2.6	-(13.6±2.6)	172±2.6	0.987
3-ethyl-3-pentanol	6.4±2.1	13.8±0.8	11.3±0.8	-(27.2±2.7)	19.4±1.2	0.979
1,2-Ethanediol	0.4±0.1	7.8±0.7	5.3±0.7	-(49.6±2.4)	20.1±1.0	0.951
1,2-Propanediol	0.5±0.1	8.2±0.6	5.7±0.6	-(48.6±2.2)	20.2±0.9	0.964
1,2-Butanediol	0.9±0.2	8.8±0.7	6.3±0.7	-(43.9±2.3)	19.4±1.0	0.966
1,6-Hexanediol	4.9±1.6	11.3±0.8	8.8±0.8	-(29.5±2.8)	17.6±1.2	0.968
1,7-Heptanediol	7.8±2.8	12.2±0.9	9.7±0.9	-(25.5±3.0)	17.4±1.3	0.969
1,8-Octanediol	31.8±4.5	15.6±1.1	13.2±1.1	-(13.9±3.8)	17.3±1.6	0.969
1,9-Nonanediol	14.8±2.5	13.5±0.4	11.0±0.4	-(20.2±1.4)	17.0±0.6	0.994
1,10-Decanediol	26.2±7.6	14.8±0.7	12.3±0.7	-(15.5±2.4)	16.9±1.0	0.986
Cyclohexanol	15.2±6.0	14.8±1.2	12.3±1.2	-(20.0±3.8)	18.3±1.6	0.965
trans-1,2-Cyclohexanediol	5.1±2.0	12.7±1.0	10.2±1.0	-(29.1±3.2)	18.9±1.4	0.966
exo-Norborneol	6.9±2.0	14.5±1.4	12.0±1.4	-(26.6±4.8)	19.9±2.0	0.943
cis-2-Methylcyclohexanol	18.4±5.1	14.5±1.4	12.1±1.4	-(18.4±4.1)	17.5±1.7	0.959
(+)-Fenchol	21.6±7.9	16.3±0.9	13.8±0.9	-(17.1±3.0)	18.9±1.3	0.982
(+)-Borneol	12.4±3.5	14.5±1.1	12.1±1.1	-(21.7±3.6)	18.5±1.5	0.967
(−)-Menthol	37.4±4.8	16.9±1.0	14.4±1.0	-(12.5±3.3)	18.1±1.4	0.980
(±)-*exo*,*exo*-2,3-Camphanediol	17.2±5.1	14.9±1.0	12.4±1.0	-(19.0±3.4)	18.1±1.4	0.972
(1S,2S,3R,5S)-(+)-Pinanediol	43.4±10.1	17.3±1.3	14.8±1.3	-(11.3±4.2)	18.2±1.8	0.966

[a]Squared coefficients of determination for the obtained Arrhenius plots

https://doi.org/10.5194/egusphere-2023-1381
Preprint. Discussion started: 14 August 2023

The values of E_a increased following the increase in the length of the carbon backbone (Table 2), before reaching the average value of approx. 15 (kJ × mol^{-1}), which is likely due to increasing diffusion contribution for higher-MW AAs (Table S3) (Schöne et al., 2014; Sarang et al., 2021). In solution, the rate of reaction is diffusion-limited if every encounter between reactants (here AAs and OH) leads to a reaction (Sarang et al., 2021). Consequently, the E_a for the aqueous reactions with a high diffusion contribution is approx. 15 (kJ × mol^{-1}) (Ervens et al., 2003), due to the temperature-dependence of the viscosity of water, which also follows the Arrhenius relationship.

For AAs under investigation, the values of $\Delta S^{\ddagger}$ increased with the increasing length of the carbon backbone; negative $\Delta S^{\ddagger}$ values were obtained for all AAs (Table 2). The $\Delta G^{\ddagger}$ values obtained were all in the same order, indicating the same transition state and reaction mechanism (Ervens et al., 2003). The average $\Delta G^{\ddagger}$ of approx. 20 kJ/mol obtained here (Table 2) is very similar to the previously reported values, for the reaction of OH with aliphatic, oxygenated molecules (Ervens et al., 2003; Hoffmann et al., 2009; Otto et al., 2018; Schaefer et al., 2020; Witkowski et al., 2021). For all AAs under investigation, positive $\Delta H^{\ddagger}$ values, between 4 and 15 (kJ/mol) were obtained. [51, 53] Therefore, the values of activation parameters obtained in this work confirm a predominance of the H-atom abstraction mechanism (Ervens et al., 2003; Otto et al., 2018; Schaefer et al., 2020; Witkowski et al., 2021).

AAs with -OH moieties separated by more than one carbon atom were characterized by a noticeably higher OH reactivity as compared with the vicinal poly(alcohol)s - Fig. 6 (Hoffmann et al., 2009).

https://doi.org/10.5194/egusphere-2023-1381
Preprint. Discussion started: 14 August 2023

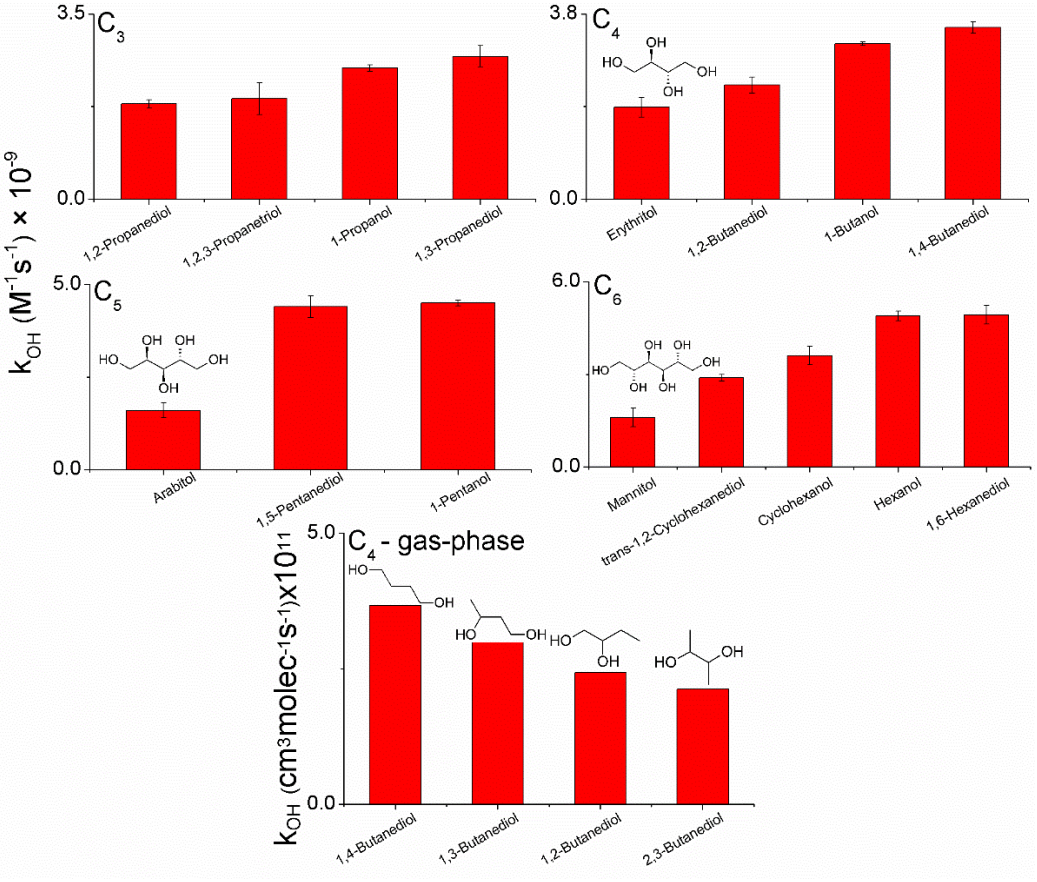

Figure 6: Measured k_{OH} values (this work and literature data) for the selected mono and poly(alcohols).

As previously reported, the -OH moieties in 1,2-diols most likely interact via polarization and electrostatic effects, rather than forming intramolecular hydrogen bonds (Klein, 2003; Das et al., 2015). Such interactions may affect the mesomeric donor effect of -OH (Monod and Doussin, 2008), thereby resulting in the observed decrease in the measured $k_{OH_{aq}}$ values for the vicinal poly(alcohol)s. A limited number of $k_{OH_{gas}}$ values available in the literature for poly(alcohol)s – Fig. 6 - also supports this hypothesis (McGillen et al., 2020).

The experimental data acquired in this work, and the literature data (Buxton et al., 1988; McGillen et al., 2020; M. R. McGillen, 2021), revealed noticeably lower $k_{OH_{aq}}$ values for reaction with the cyclic alcohols and hydrocarbons as compared with their linear analogs (Fig. 7).

https://doi.org/10.5194/egusphere-2023-1381
Preprint. Discussion started: 14 August 2023

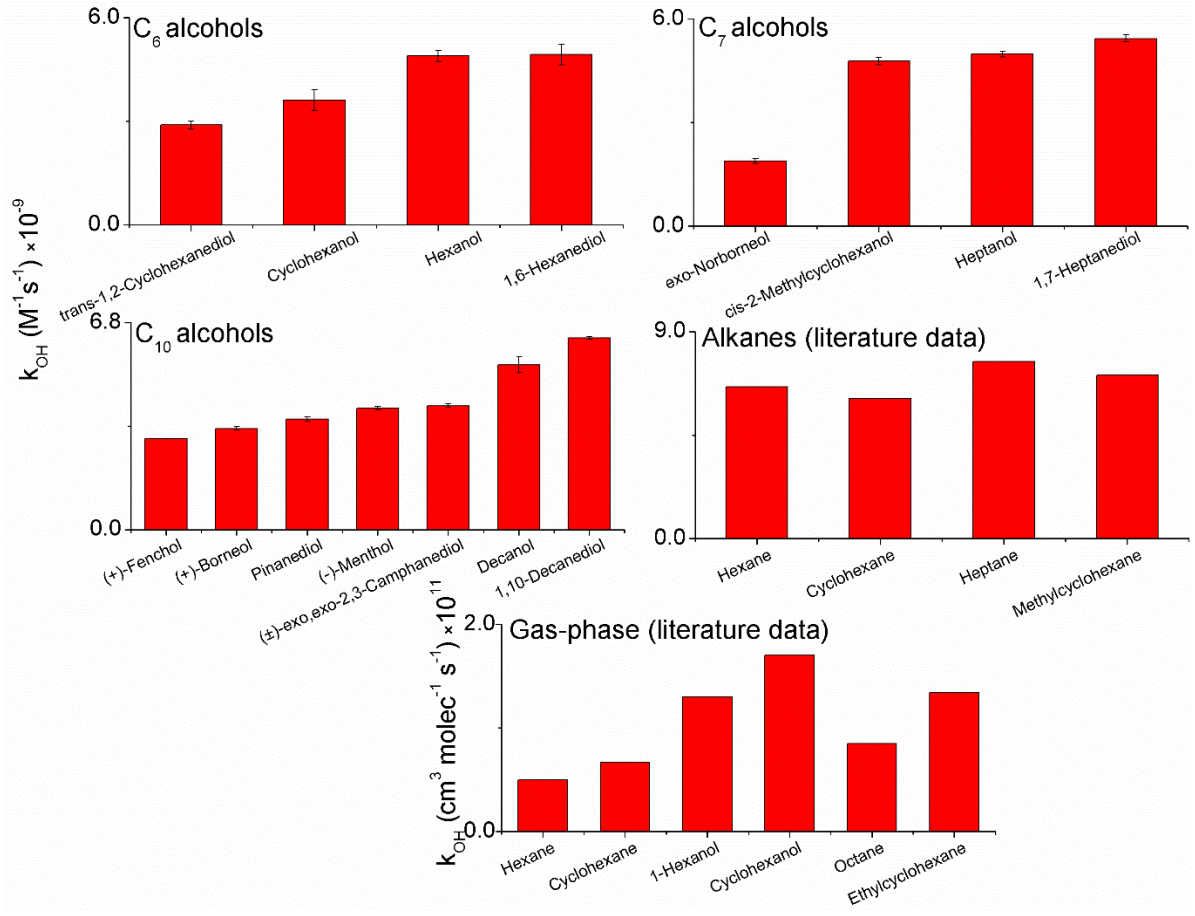

Figure 7: k_{OH} values measured for cyclic (C_6) and linear alcohols in the gas and aqueous phases.

At the same time, the opposite trend is observed in the gas phase (Fig 7) for the C_6-C_8 alcohols and alkanes (Atkinson, 1986b, 1987). This may be caused by the different mobility of the linear and cyclic reactants inside the water cage, resulting in a different intramolecular selectivity of OH (Kopinke and Georgi, 2017). However, more experimental data are needed to provide more insights into the reactivities of the aliphatic WSOCs containing strained and non-strained aliphatic rings towards OH; for instance, the $k_{OH_{aq}}$ measured here for *cis*-2-methylcyclohexanol does not follow this general trend (Fig. 7).

3.2 Structure-activity relationship

The $k_{OH_{aq}}$ values measured in this work at 298K, and the literature data (section 2.5), were used to optimize F and G factors only for CH_2 and -OH moieties (Model 1) or substituent factors for CH_3, CH_2, CH, and -OH, moieties, C_4-C_6 rings and the base (partial) rate coefficients (Model 2) – Table 3. Model 2 also included a new substituent factor for molecules with straight-chain carbon backbones - F $\geq(CH_2)_6$ - see also Fig. 1.

https://doi.org/10.5194/egusphere-2023-1381
Preprint. Discussion started: 14 August 2023

Table 3. SAR (Model 2) substituent factors and base rate coefficients

Group	Substituent factors		Ref.
	F	G	
CH_3	1.40	1.16	This work
CH_2	1.34	1.00	This work
CH	1.03	1.05	This work
$\geq(CH_2)_6$	0.76		This work
C	1.00	1.00	(Monod and Doussin, 2008)
OH	1.97	0.56	This work
C_6	0.65		This work
C_5	0.61		This work
C_4	1.34		This work
FC=O	0.20	0.90	(Doussin and Monod, 2013)
COOH	0.16	0.59	(Witkowski et al., 2021)
COO-	0.54	0.64	(Witkowski et al., 2021)
Base (partial) rate coefficients, (k_{OH}) at 298K×10^{-8}			
k_{CH3}	4.06		
k_{CH2}	6.17		This work
k_{CH}	4.40		
k_{OH}	1.54		
Temperature-dependence of the base rate coefficients			
	C×10^{-3}, ($M^{-1}s^{-1}$)	D×10^{-2}, (K)	
k_{CH3}	5.50	0.55	
k_{CH2}	197.9	9.98	This work
k_{CH}	5.04	0.05	
k_{OH}	1.74	0.01	

The unadjusted SAR included the neighboring parameters and partial rate coefficients originally derived by (Monod and Doussin, 2008; Doussin and Monod, 2013), and F and G factors for carboxylic acids and carboxylate ions recently updated by our group (Witkowski et al., 2021). Note also that *cis*-pinonic acid was the only carbonyl compound in the kinetic dataset used to optimize SAR parameters (1). As demonstrated in our previous study, hydration (formation of gem-diol) of *cis*-pinonic acid is negligible (Witkowski et al., 2021).

https://doi.org/10.5194/egusphere-2023-1381
Preprint. Discussion started: 14 August 2023

In Table 3, the F and G values >1 indicate activation whereas values <1 correspond to the deactivating effect of a given group (Kwok and Atkinson, 1995). Furthermore, the values of F and G factors are often rationalized via the field and resonance effects, which are expressed by the values of (*R*, resonance) and (*F*, field) parameters defined by (Swain and Lupton, 1968). The resonance effects primarily affect the α-position whereas the field effects are associated with the β-positions (Monod and Doussin, 2008). In Table 4, the negative values correspond to the electron-donating group (activating effect) whereas positive values indicate deactivation (electron withdrawing). Consequently, alkyl substituents should exhibit activating effects in both α and β-position following their negative values of F and R parameters, whereas α-activation and β-deactivation are expected for -OH (Table 4).

Table 4. Selected resonance (R) and field (F) factors; negative values correspond to activating effects and positive values indicate deactivation

Group	Resonance effects (R, α-position)	Field effects (F, β-position)
-OH	-1.89	0.46
CH_3	-0.41	-0.1
CH_3CH_2	-0.44	-0.2

In Model 1, the F and G factors of 1.40 (F), 0.63 (G) for -CH_2, and 1.51 (F) and 0.81(G) for -OH were obtained, what only resulted in a moderate improvement of the SAR accuracy (Fig. 8B), even though a majority of model compounds (Table 1) possessed both of these moieties, which should result in a reliable model fit (Peduzzi et al., 1996).

https://doi.org/10.5194/egusphere-2023-1381
Preprint. Discussion started: 14 August 2023

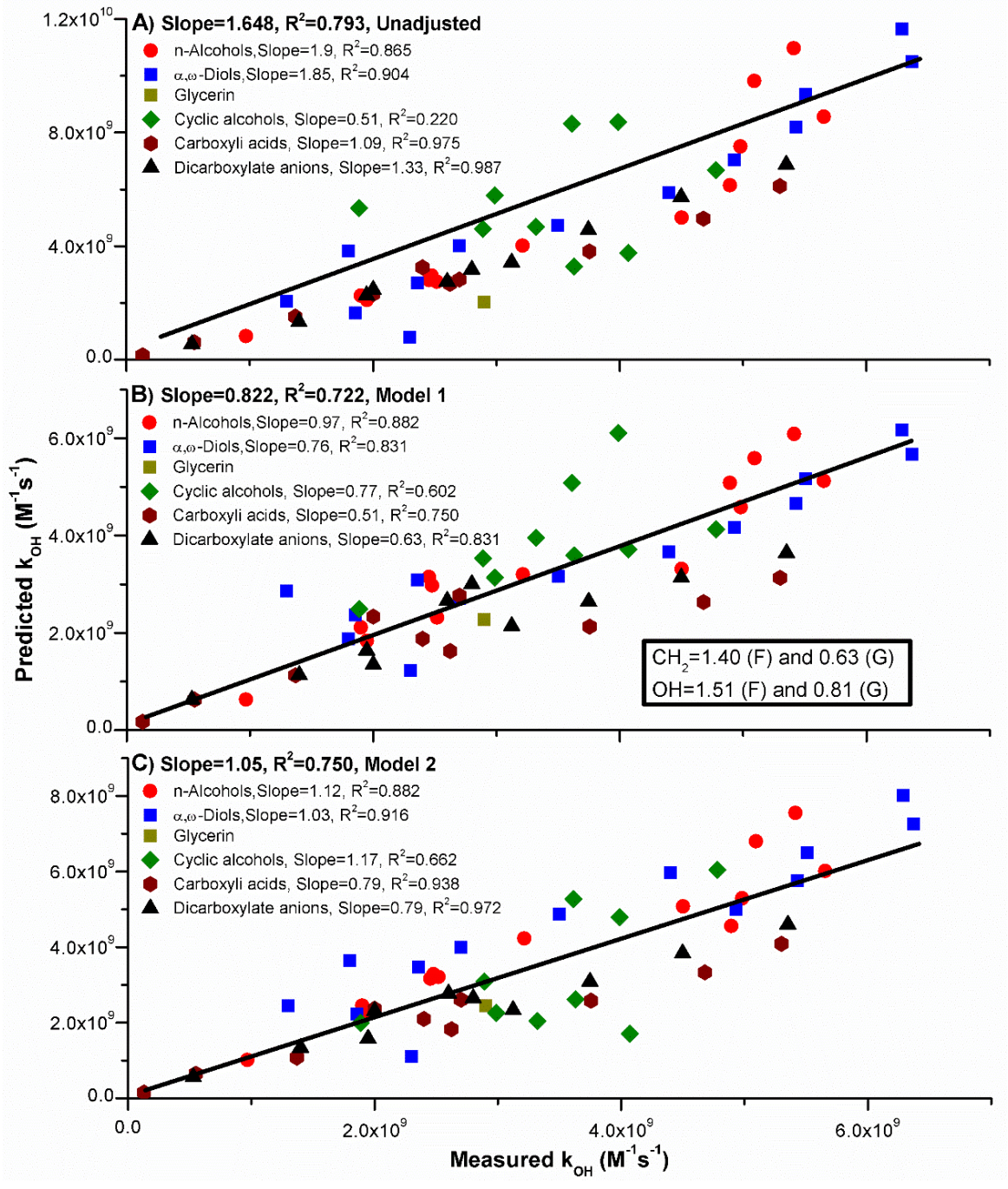

Figure 8: Accuracies of unadjusted (A), and adjusted (B, model 1) and (C, model 2) SARs for alcohols and carboxylic acids at 298K.

The values obtained for -OH (Model 1) are similar to the previously reported values (Monod and Doussin, 2008). but the strong β-deactivating effect of CH_2 (Fig. 8B) is difficult to explain, especially taking into account the field and resonance

https://doi.org/10.5194/egusphere-2023-1381
Preprint. Discussion started: 14 August 2023

effects for alkyl substituents (Table 4). Such behavior of Model 1 most likely reflects the trends in OH reactivities observed for the homolog series of linear alcohols and diols in the aqueous phase (Figs. 4 and 5).

By only adjusting the F and G factors for -OH and CH_2, it was impossible to further improve the performance of the model. Moreover, the accuracy of Model 1 was higher for AAs but significantly lower for carboxylic acids and carboxylate ions (Fig. 8B). In an attempt to further improve the model, all substituent factors and partial rate coefficients were adjusted. The resulting SAR parameters showed very little correlation with the factors proposed by Swain and Lupton (results not shown). At the same time, only a minor improvement in the SAR performance was achieved, but the G-parameter obtained for CH_2 was always <1.

The original SAR developed by Monod and Doussin was based on the values of $k_{OH_{aq}}$ measured primarily for the lower-MW molecules, which is reflected by the large positive bias of the unadjusted model (slope=1.648, Fig. 8A), especially for the longer-chain AAs (Monod and Doussin, 2008; Doussin and Monod, 2013). Consequently, using this methodology, which was originally developed for predicting the values of $k_{OH_{gas}}$, an adequate representation of the aqueous OH reactivity of higher-MW molecules in the aqueous phase is very challenging.

For this reason, it was concluded that there is a need for an additional parametrization of the observed reactivity of the WSOCs with larger carbon backbones (Fig. 5). Therefore, a new F factor, reflecting the reactivities of the longer chain molecules, was introduced (Table 3) - see also Fig. 1. In Model 2, the partial k_{OH} of every CH_2 moiety is additionally adjusted for the C_6 and longer-chain precursors, which resulted in a noticeably higher accuracy of SAR (Fig.8C). Following this adjustment, the versatility, and accuracy of Model 2 were noticeably improved, resulting in the better performance of the model for alcohols, diols and carboxylic acids and carboxylate anions (Fig. 8C). Accuracy of SAR (Model 2) was lowest for cyclic alcohols (Fig. 8B), even though almost all predicted $k_{OH_{aq}}$ values agreed, within the factor of 2, with the experimental data. The F-factors <1 obtained for the C_5 and C_6-rings reflects the lower OH reactivates observed in this work for the cyclic AAs (Fig. 7).

In Model 2, the adjusted values of the neighboring parameters and partial rate coefficients for the alkyl groups (CH_3, CH_2, and CH) – Table 3 - are all in good agreement with the previously reported data (Monod and Doussin, 2008). Furthermore, the substituent factors derived for -OH are also in very good agreement with the literature data and correlate well with the resonance and field effects of the hydroxyl moiety (Table 4). The value of the partial rate coefficient for the abstraction of H-atom from the -OH was approx. three times lower than the rates obtained for the CH_n groups (Table 2), thereby confirming that a direct abstraction of H-atom from -OH is a minor reaction pathway (Atkinson, 1986a; Kwok and Atkinson, 1995; Monod and Doussin, 2008).

The optimized SAR (Model 2) was used to obtain the values of C and D factors, which allows for predicting the temperature-dependent $k_{OH_{aq}}$ values for AAs and carboxylic acids (eq. IV and V); similar performances of the model were obtained for all temperatures (Table S6).

https://doi.org/10.5194/egusphere-2023-1381
Preprint. Discussion started: 14 August 2023

4 Atmospheric implications

4.1 Lifetimes of terpenoic alcohols

The lifetimes for the five TAs investigated in this work were estimated with eq. VI. (Sarang et al., 2021)

$$\tau = \frac{1}{\left(\frac{k_{OH_{gas}}}{H_{OH}^{cc}} + k_{OH_{aq}} H_{AA}^{cc} \omega\right)[OH]_{aq}} \qquad (VI)$$

In eq. VI, τ is the combined lifetime in the gas and the aqueous phase due to the reaction with the OH. Therefore, this approach considers both gas and aqueous oxidation of AAs by the OH and their relative importance, depending on Henry's law equilibria and LWC in a given air mass (Sarang et al., 2021).

In eq. VI, $k_{OH_{gas,}}$ and $k_{OH_{aq}}$ are the bimolecular reaction rate coefficients for the reaction of a given AA in the gas and aqueous phase with the OH ($M^{-1}s^{-1}$) at 298K respectively. H_{OH}^{cc} and H_{AA}^{cc} are the dimensionless Henry's law constants for the OH (H_{OH}^{cc}) and for the given AA (H_{AA}^{cc}) (Sander, 2015), ω is the liquid water content (LWC, m^3/m^3), $[OH]_{aq}$ is the aqueous concentration of OH (M). In eq. VI, the gas-phase OH concentration is connected with $[OH]_{aq}$ via Henry's equilibrium, assuming that there are no additional sources of OH; the average reported H_{OH}^{cc} = 764 was used (Sander, 2015).

Table 5. Data used to estimate the atmospheric lifetimes of the five terpenoic alcohols due to reaction with the OH at 298K

Name	$k_{OH_{aq}}\times10^{-9}$ $(M^{-1}s^{-1})$[a]	$k_{OH_g}\times10^{11}$ $(cm^3molec^{-1}s^{-1})$	Ref.	H^{cc}	Ref.
Fenchol	2.99	2.49	(McGillen et al., 2020; McGillen et al., 2021)	5.0×10^3	(Fichan et al., 1999)
Borneol	3.32	2.65		5.08×10^3	(Sander, 2015)
Menthol	3.99	1.48		1.20×10^3	(Sander, 2015)
Camphanediol	4.07	2.78	(Atkinson, 1986b; Kwok and Atkinson, 1995)	4.46×10^8	
Pinanediol	3.63	2.12		6.75×10^8	(EPISuite4.11)

[a] $k_{OH_{aq}}$ values measured in his work

The $k_{OH_{aq}}$ values measured in this work were used to calculate the τ for the five TAs. For pinanediol, the $k_{OH_{gas}}$ value was predicted with SAR due to a lack of measured values. Likewise, when possible, the experimentally measured $k_{OH_{gas}}$ and H_{AA}^{cc} values were used; otherwise, the values listed were estimated with structure-activity relationship (SAR) (Atkinson, 1986b; Kwok and Atkinson, 1995), and with HenryWin (Table 5).

The τ values were calculated as a function of LWC and $[OH]_{aq}$; the dotted lines in Fig. 9 represent the range of OH in different types of aqueous particles (Herrmann et al., 2010). The y-axis (Fig. 9) represents the total lifetime (τ, h). The plateaus

https://doi.org/10.5194/egusphere-2023-1381
Preprint. Discussion started: 14 August 2023

regions, corresponding to the lower values of LWC, indicate that the reaction with the OH takes place almost exclusively in the gas phase. In terms of interactions with liquid water in the atmosphere, the values of τ <20 h are most relevant because an air parcel spends approx. 18 h inside a cloud (Herrmann et al., 2015).

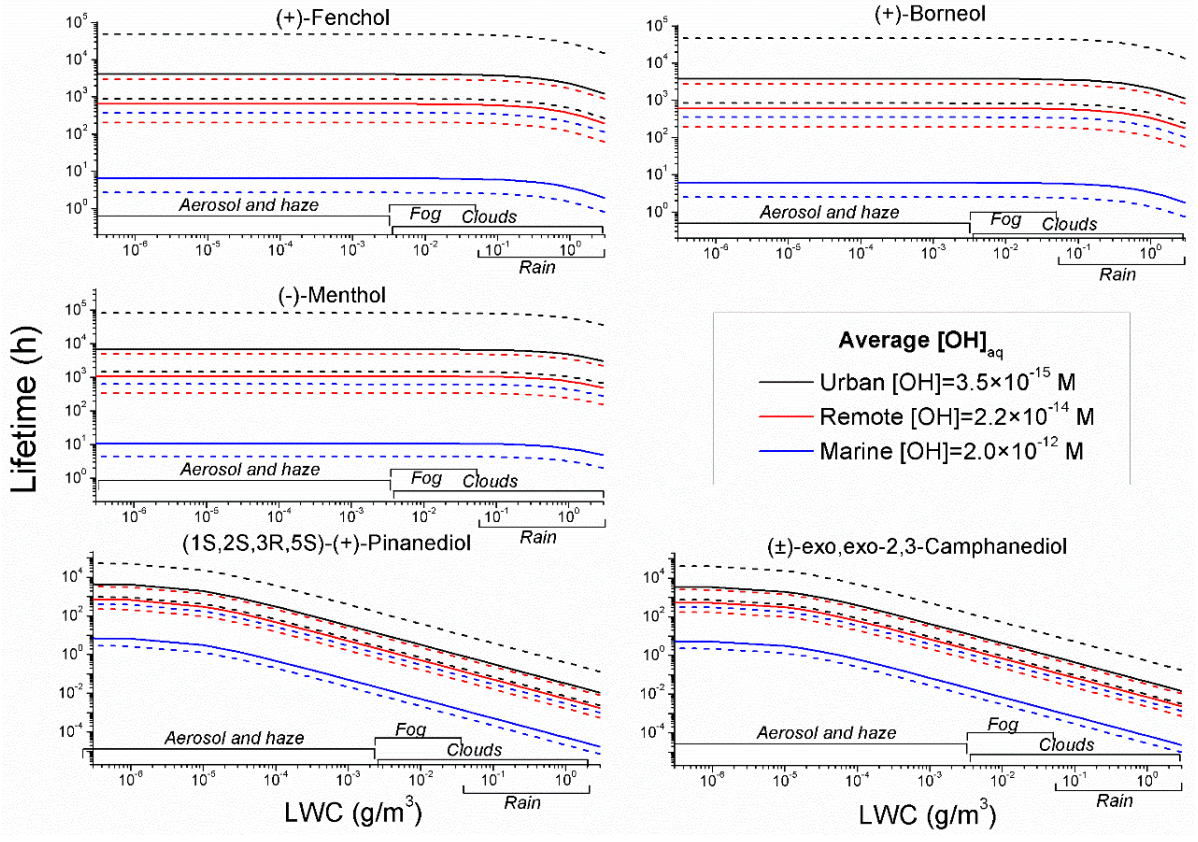

Figure 9: The estimated lifetimes of TAs. The dotted lines represent lifetimes corresponding to the minimum and maximum $[OH]_{aq}$ in different aqueous particles.

The new $k_{OH_{aq}}$ values acquired in this work indicate that TAs are likely to undergo aqueous oxidation in clouds (LWC≥0.1 g/m^3) whereas terpenoic diols will react with the OH in aqueous aerosols, clouds, and fogs (LWC≥10^{-4} g/m^3) with the estimated lifetimes < 1min – Fig. 9.

The reaction of OH with terpenoic acids has been receiving considerable attention in connection with the formation of $_{aq}$SOAs (Aljawhary et al., 2016; Zhao et al., 2017; cis-Pinonic Acid Oxidation by Hydroxyl Radicals in the Aqueous Phase under Acidic and Basic Witkowski and Gierczak, 2017; Otto et al., 2018; Witkowski et al., 2018b; Witkowski et al., 2018a, 2019; Amorim et al., 2020; Amorim et al., 2021; Witkowski et al., 2021). Using the same approach (eq. VI) we have recently derived τ values for six terpenoic acids, identified as the major components of unaged α-pinene SOA (Witkowski et al., 2023). It was concluded that *cis*-pinic, *cis*-pinonic, hydroxypinonic, and oxopinonic acids will undergo a reaction with the OH in the aqueous phase LWC is ≥ 1×10^{-3} (g/m^3). Hence, in the case of terpenoic diols (Fig. 9), their potential to undergo aqueous oxidation

https://doi.org/10.5194/egusphere-2023-1381
Preprint. Discussion started: 14 August 2023

under realistic atmospheric conditions is comparable with some terpenoic acids. In the case of *cis*-pinonic acid, the measured mass yields of $_{aq}$SOAs following the reaction with the OH were as high as 60%. (Aljawhary et al., 2016) At the same time, to date, little mechanistic data is available about the formation of low-volatility products from TAs following RI.

Global emissions of oxygenated terpenes are tentatively estimated at 26 ($TgC \times yr^{-1}$) (Sindelarova et al., 2014). TAs are emitted by vegetation (Héral et al., 2021), but are also used in the industry, as fragrance agents and solvents.(Belsito et al., 2008) Therefore, TAs, and especially terpenoic diols, are potentially important precursors of $_{aq}$SOAs in both urban and remote environments.

4.2 Influence of the temperature

The values of H^{cc}, $k_{OH_{aq,}}$ and $k_{OH_{gas}}$ all depend on the temperature. In a relatively narrow temperature range, in which liquid water exists in the atmosphere, the enthalpy of dissolution $\left(\frac{dln(H)}{d1/T}\right)$ can be considered constant (Sander, 2015). Hence, the Van't Hoff equation can be applied to describe the temperature-dependence of H^{cc} values (Sander, 2015). For instance, a decrease in the temperature by 20° will result in a 2 to 7-fold increase of the H^{cc} values of TAs and OH (Sander, 2015). Consequently, a significantly higher fraction of these reactants will reside in the aqueous phase at lower temperatures, thereby strongly favoring the aqueous chemical aging of TAs in the atmosphere.

The data acquired in this work, and the literature data (1) confirm that the temperature dependence of the $k_{OH_{aq}}$ values for the TAs follow the Arrhenius relationship. Considering the temperature range in which liquid water exists in the atmosphere, the same conclusion also applies to the temperature dependence of the $k_{OH_{gas}}$ values for TAs and similar molecules. Furthermore, the values of E_a and A (section 2.4) measured in this work, as well as literature data, show relatively similar temperature dependencies of $k_{OH_{aq}}$ and $k_{OH_{gas}}$(Atkinson, 1986a; Kwok and Atkinson, 1995; Herrmann, 2003; Hoffmann et al., 2009; McGillen et al., 2020). Hence, the $k_{OH_{aq}}/k_{OH_{gas}}$ ratio for the TAs (Table 5) will remain mostly unchanged in the considered temperature range. At the same time, a lower temperature will result in a lower oxidation rate, thereby decreasing the τ values, which can make other removal mechanisms more relevant.

These conclusions are valid primarily for cloud water droplets which are diluted and, more often than not, can be treated as ideal solutions (Herrmann, 2003; Richters et al., 2015). On the other hand, the ionic strength (I) of some aerosols can be as high as 43 (M) (Cheng et al., 2016). The high I values of some aerosols will affect the kinetics of RI, partitioning, and rates of diffusion of the reactants (Mekic and Gligorovski, 2021). While salting-out of organics will likely occur in aqueous particles with high I value, salts are also expected to enhance the rate of RI (Zhou et al., 2019).

https://doi.org/10.5194/egusphere-2023-1381
Preprint. Discussion started: 14 August 2023

4.4 Potential formation of $_{aq}$SOAs from terpenoic alcohols

No product studies were carried out in this work. Nevertheless, as indicated by the new kinetic data acquired in this work, the cyclic TAs investigated should be considered as the potential precursors of $_{aq}$SOAs. For instance, cyclic terpenes are often more efficient at forming SOAs as compared to the linear precursors (Lim and Ziemann, 2009; Hunter et al., 2014). Following RI, oxygenated functional groups are added to the original carbon backbone of the precursor, accordingly to Russell's and Bennett-Summer's mechanisms (Russell, 1957; Bennett and Summers, 1974). Alkoxy (RO) radicals are formed from the reaction of an alkyl radical with O_2 via the decomposition of tetroxide intermediates (Bennett and Summers, 1974; von Sonntag and Schuchmann, 1991). At the same time, in the case of linear precursors, the β-scission reaction of RO radicals can result in a decreased length of the carbon backbone (Rauk et al., 2003; Enami and Sakamoto, 2016; Murakami and Ishida, 2017). Consequently, β-scission involving non-cyclic precursors results in lower MW and, more volatile products, that are less likely to contribute to SOAs (Rauk et al., 2003; Enami and Sakamoto, 2016; Murakami and Ishida, 2017). Hence, the cyclic precursors, such as TAs, are likely to yield highly-oxidized, low-volatility following reaction with the OH without undergoing too much fragmentation (Claeys et al., 2009; Ceacero-Vega et al., 2012; Sato et al., 2016).

5 Conclusions and further work

Utilizing a bulk photoreactor combined with the off-line quantification of the changing alcohol concentrations using gas chromatography allowed us to obtain $k_{OH_{aq}}$ for multiple compounds from a single experiment (Herrmann et al., 2005). This method is significantly less laborious as compared with some of the other methods of measuring $k_{OH_{aq}}$, and can be used to obtain large kinetic datasets, thereby facilitating the expansion of the current kinetic databases for environmentally-widespread WSOCs.

The measured $k_{OH_{aq}}$ values for AAs (this work and literature data) revealed that it was necessary to introduce an additional neighboring parameter to further improve the performance of the predictive model of the linear, longer chain ($\geq C_6$) molecules. The need to modify the methodology used in the original SAR was most likely connected with a different transition state formed between OH and AAs in the gas and in the aqueous phases (Smith and Ravishankara, 2002; Mellouki et al., 2003; Herrmann et al., 2005). It is still unclear if the new, modified SAR is capable of accurately predicting the values of $k_{OH_{aq}}$ for the homolog series of different oxygenated molecules, including carbonyls, esters, linear acids, and multifunctional molecules. More kinetic data for higher-MW molecules with larger carbon backbones, including also polyfunctional compounds, are needed to further improve the capabilities of kinetic SARs.

Models utilized for generating explicit oxidation schemes of atmospherically-abundant organics frequently rely on kinetic SARs to derive rate coefficients and branching ratios of the numerous by-products involved in a given mechanism (Bräuer et al., 2019). Hence, further expanding the applicability domain of the aqueous kinetic SARs will improve our ability to predict the effects of various, multiphase processes (like for instance formation and aging of $_{aq}$SOAs) on air quality, climate, and

https://doi.org/10.5194/egusphere-2023-1381
Preprint. Discussion started: 14 August 2023

public health. Likewise, the dependence of the $k_{OH_{aq}}$ values for I also need to be further investigated to provide some insights into the time scales of RI, and other radical reactions, in the presence of high amounts of salts (Herrmann et al., 2015).

The values of neighboring parameters in SAR for strained and non-strained rings are still somewhat ambiguous, again due to the very limited number of experimentally measured $k_{OH_{aq}}$ values for such molecules. However, the results obtained in this work also indicate that there might be significant differences in the reactivities of such molecules in the gas and aqueous phases towards OH. The updated SAR also showed good accuracy in the temperature range between 278-328K, which underlines the need to further expand the kinetic databases, listing the temperature-dependent $k_{OH_{aq}}$ values.

The atmospheric lifetimes estimated for the five TAs - fenchol, borneol, menthol, camphanediol, and pinanediol – underlined the need to further investigate other non-acidic precursors of $_{aq}$SOAs in the atmosphere. Recently, in connection with the formation of $_{aq}$SOAs, a lot of attention has been dedicated to studying acidic precursors, primarily terpenoic acids. Higher-MW organic acids are expected to reside almost entirely in the aqueous phase, even at relatively low values of LWC. Likewise, all TAs, and especially diols, studied in this work can undergo RI in clouds, fogs, and wet aerosols under realistic atmospheric conditions, which underlines the need to study the formation of low-volatility products from such precursors.

In the atmosphere, a decrease in the temperature will strongly promote the partitioning of organics into the aqueous phase, due to the temperature dependence of the Henry's Law constants. At the same time, a decrease in the temperature lowers the $k_{OH_{aq}}$ values, thereby decreasing the rate of RI.

Appendices

(1) Kinetic datasets of the $k_{OH_{aq}}$ values for alcohols, diols, carboxylic acids, and carboxylate ions measured at 298K and in the temperature range between 278 and 328 K; this work and literature data.

Credit author statement

Bartłomiej Witkowski: Conceptualization, Supervision, Original Draft, Data Curation, Methodology, Writing - Review & Editing. Priyanka Jain: Investigation, Formal analysis, Methodology, Validation, Data Curation, Writing - Review & Editing. Beata Wileńska: Methodology, Resources. Tomasz Gierczak: Project administration, Supervision, Funding acquisition, Resources, Writing - Review & Editing.

Declaration of competing interest

The authors have no competing interests to declare

https://doi.org/10.5194/egusphere-2023-1381
Preprint. Discussion started: 14 August 2023

Acknowledgments

This project was funded by the Polish National Science Centre: grant number 2018/31/B/ST10/01865. This study was carried out at the Biological and Chemical Research Centre, the University of Warsaw, established within the project co-financed by the European Union from the European Regional Development Fund under the Operational Programme Innovative Economy, 2007 – 2013.

References

1, A.: [dataset], https://docs.google.com/spreadsheets/d/1pyktOxm3frLfxxfVoFk1eIzJZx-75VMZ/edit?usp=sharing&ouid=118379828045942672528&rtpof=true&sd=true,

Adams, G., Boag, J., Currant, J., and Michael, B.: Absolute rate constants for the reaction of the hydroxyl radical with organic compounds, 131-143, https://doi.org/10.1063/1.444367, 1965.

Aljawhary, D., Zhao, R., Lee, A. K. Y., Wang, C., and Abbatt, J. P. D.: Kinetics, Mechanism, and Secondary Organic Aerosol Yield of Aqueous Phase Photo-oxidation of α-Pinene Oxidation Products, J. Phys. Chem. A, 120, 1395-1407, https://doi.org/10.1021/acs.jpca.5b06237, 2016.

Amorim, J. V., Guo, X., Gautam, T., Fang, R., Fotang, C., Williams, F. J., and Zhao, R.: Photo-oxidation of pinic acid in the aqueous phase: a mechanistic investigation under acidic and basic pH conditions, 1, 276-287, https://doi.org/10.1039/D1EA00031D, 2021.

Amorim, J. V., Wu, S., Klimchuk, K., Lau, C., Williams, F. J., Huang, Y., and Zhao, R.: pH Dependence of the OH Reactivity of Organic Acids in the Aqueous Phase, 54, 12484-12492, https://doi.org/10.1021/acs.est.0c03331, 2020.

Anbar, M., Meyerstein, D., and Neta, P.: Reactivity of aliphatic compounds towards hydroxyl radicals, 742-747, https://doi.org/10.1039/J29660000742, 1966.

Atkinson, R.: Estimations of OH radical rate constants from H-atom abstraction from CH and OH bonds over the temperature range 250-1000 K, 18, 555-568, https://doi.org/10.1002/kin.550180506, 1986a.

Atkinson, R.: Kinetics and mechanisms of the gas-phase reactions of the hydroxyl radical with organic compounds under atmospheric conditions, Chem. Rev, 86, 69-201, https://doi.org/10.1021/cr00071a004, 1986b.

Atkinson, R.: A structure-activity relationship for the estimation of rate constants for the gas-phase reactions of OH radicals with organic compounds, 19, 799-828, https://doi.org/10.1002/kin.550190903, 1987.

Belsito, D., Bickers, D., Bruze, M., Calow, P., Greim, H., Hanifin, J. M., Rogers, A. E., Saurat, J. H., Sipes, I. G., and Tagami, H.: A toxicologic and dermatologic assessment of cyclic and non-cyclic terpene alcohols when used as fragrance ingredients, 46, S1-S71, https://doi.org/10.1016/j.fct.2008.06.085, 2008.

Bennett, J. E. and Summers, R.: Product Studies of the Mutual Termination Reactions of sec-Alkylperoxy Radicals: Evidence for Non-Cyclic Termination, 52, 1377-1379, https://doi.org/10.1139/v74-209, 1974.

Bräuer, P., Mouchel-Vallon, C., Tilgner, A., Mutzel, A., Böge, O., Rodigast, M., Poulain, L., van Pinxteren, D., Wolke, R., Aumont, B., and Herrmann, H.: Development of a protocol for the auto-generation of explicit aqueous-phase oxidation schemes of organic compounds, 19, 9209-9239, https://doi.org/10.5194/acp-19-9209-2019, 2019.

https://doi.org/10.5194/egusphere-2023-1381
Preprint. Discussion started: 14 August 2023

Buxton, G. V., Greenstock, C. L., Helman, W. P., and Ross, A. B.: Critical Review of rate constants for reactions of hydrated electrons, hydrogen atoms and hydroxyl radicals (OH/O- in Aqueous Solution, 17, 513-886, https://doi.org/10.1063/1.555805, 1988.

Carlton, A. G., Christiansen, A. E., Flesch, M. M., Hennigan, C. J., and Sareen, N.: Multiphase Atmospheric Chemistry in Liquid Water: Impacts and Controllability of Organic Aerosol, 53, 1715-1723, https://doi.org/10.1021/acs.accounts.0c00301, 2020.

Ceacero-Vega, A. A., Ballesteros, B., Bejan, I., Barnes, I., Jiménez, E., and Albaladejo, J.: Kinetics and Mechanisms of the Tropospheric Reactions of Menthol, Borneol, Fenchol, Camphor, and Fenchone with Hydroxyl Radicals (OH) and Chlorine Atoms (Cl), 116, 4097-4107, https://doi.org/10.1021/jp212076g, 2012.

Chen, H., Su, X., He, J., Zhang, P., Xu, H., and Zhou, C.: Investigation on combustion characteristics of cyclopentanol/diesel fuel blends in an optical engine, 167, 811-829, https://doi.org/10.1016/j.renene.2020.11.155, 2021.

Cheng, Y., Zheng, G., Wei, C., Mu, Q., Zheng, B., Wang, Z., Gao, M., Zhang, Q., He, K., Carmichael, G., Pöschl, U., and Su, H.: Reactive nitrogen chemistry in aerosol water as a source of sulfate during haze events in China, 2, e1601530, https://doi.org/10.1126/sciadv.1601530, 2016.

cis-Pinonic Acid Oxidation by Hydroxyl Radicals in the Aqueous Phase under Acidic and Basic Witkowski, B. and Gierczak, T.: cis-Pinonic Acid Oxidation by Hydroxyl Radicals in the Aqueous Phase under Acidic and Basic Conditions: Kinetics and Mechanism, 51, 9765-9773, https://doi.org/10.1021/acs.est.7b02427, 2017.

Claeys, M., Iinuma, Y., Szmigielski, R., Surratt, J. D., Blockhuys, F., Van Alsenoy, C., Böge, O., Sierau, B., Gómez-González, Y., Vermeylen, R., Van der Veken, P., Shahgholi, M., Chan, A. W. H., Herrmann, H., Seinfeld, J. H., and Maenhaut, W.: Terpenylic Acid and Related Compounds from the Oxidation of α-Pinene: Implications for New Particle Formation and Growth above Forests, 43, 6976-6982, https://doi.org/10.1021/es9007596, 2009.

Das, P., Das, P. K., and Arunan, E.: Conformational Stability and Intramolecular Hydrogen Bonding in 1,2-Ethanediol and 1,4-Butanediol, 119, 3710-3720, https://doi.org/10.1021/jp512686s, 2015.

Doussin, J. F. and Monod, A.: Structure–activity relationship for the estimation of OH-oxidation rate constants of carbonyl compounds in the aqueous phase, 13, 11625-11641, https://doi.org/10.5194/acp-13-11625-2013, 2013.

Enami, S. and Sakamoto, Y.: OH-Radical Oxidation of Surface-Active cis-Pinonic Acid at the Air–Water Interface, J. Phys. Chem. A, 120, 3578-3587, https://doi.org/10.1021/acs.jpca.6b01261, 2016.

Henry's law constants were calcualted with HenryWin (EPI Suite v4.11) Website: https://www.epa.gov/tsca-screening-tools/epi-suitetm-estimation-program-interface, last access Jun 20th 2023, last

Ervens, B.: Modeling the Processing of Aerosol and Trace Gases in Clouds and Fogs, 115, 4157-4198, https://doi.org/10.1021/cr5005887, 2015.

Ervens, B., Gligorovski, S., and Herrmann, H.: Temperature-dependent rate constants for hydroxyl radical reactions with organic compounds in aqueous solutions, 5, 1811-1824, https://doi.org/10.1039/B300072A, 2003.

Ervens, B., Sorooshian, A., Aldhaif, A. M., Shingler, T., Crosbie, E., Ziemba, L., Campuzano-Jost, P., Jimenez, J. L., and Wisthaler, A.: Is there an aerosol signature of chemical cloud processing?, 18, 16099-16119, https://doi.org/10.5194/acp-18-16099-2018, 2018.

Fichan, I., Larroche, C., and Gros, J. B.: Water Solubility, Vapor Pressure, and Activity Coefficients of Terpenes and Terpenoids, 44, 56-62, https://doi.org/10.1021/je980070+, 1999.

Fuzzi, S., Baltensperger, U., Carslaw, K., Decesari, S., Denier van der Gon, H., Facchini, M. C., Fowler, D., Koren, I., Langford, B., Lohmann, U., Nemitz, E., Pandis, S., Riipinen, I., Rudich, Y., Schaap, M., Slowik, J. G., Spracklen, D.

https://doi.org/10.5194/egusphere-2023-1381
Preprint. Discussion started: 14 August 2023

V., Vignati, E., Wild, M., Williams, M., and Gilardoni, S.: Particulate matter, air quality and climate: lessons learned and future needs, 15, 8217-8299, https://doi.org/10.5194/acp-15-8217-2015, 2015.
Gligorovski, S., Rousse, D., George, C., and Herrmann, H.: Rate constants for the OH reactions with oxygenated organic compounds in aqueous solution, 41, 309-326, https://doi.org/10.1002/kin.20405, 2009.
Goldstein, A. H. and Galbally, I. E.: Known and unexplored organic constituents in the earth's atmosphere, 41, 1514-1521, https://doi.org/10.1021/es072476p, 2007.
González-Sánchez, J. M., Brun, N., Wu, J., Morin, J., Temime-Roussel, B., Ravier, S., Mouchel-Vallon, C., Clément, J. L., and Monod, A.: On the importance of atmospheric loss of organic nitrates by aqueous-phase OH oxidation, 21, 4915-4937, https://doi.org/10.5194/acp-21-4915-2021, 2021.
Guenther, A., Jiang, X., Heald, C. L., Sakulyanontvittaya, T., Duhl, T., Emmons, L., and Wang, X.: The Model of Emissions of Gases and Aerosols from Nature version 2.1 (MEGAN2. 1): an extended and updated framework for modeling biogenic emissions, 5, 1471-1492, https://doi.org/10.5194/gmd-5-1471-2012, 2012.
Hallquist, M., Wenger, J. C., Baltensperger, U., Rudich, Y., Simpson, D., Claeys, M., Dommen, J., Donahue, N. M., George, C., Goldstein, A. H., Hamilton, J. F., Herrmann, H., Hoffmann, T., Iinuma, Y., Jang, M., Jenkin, M. E., Jimenez, J. L., Kiendler-Scharr, A., Maenhaut, W., McFiggans, G., Mentel, T. F., Monod, A., Prévôt, A. S. H., Seinfeld, J. H., Surratt, J. D., Szmigielski, R., and Wildt, J.: The formation, properties and impact of secondary organic aerosol: current and emerging issues, Atmos. Chem. Phys., 9, 5155-5236, https://doi.org/10.5194/acp-9-5155-2009, 2009.
Héral, B., Stierlin, É., Fernandez, X., and Michel, T.: Phytochemicals from the genus Lavandula: a review, 20, 751-771, https://doi.org/10.1007/s11101-020-09719-z, 2021.
Herrmann, H.: Kinetics of aqueous phase reactions relevant for atmospheric chemistry, 103, 4691-4716, https://doi.org/10.1021/cr020658q, 2003.
Herrmann, H., Hoffmann, D., Schaefer, T., Bräuer, P., and Tilgner, A.: Tropospheric Aqueous-Phase Free-Radical Chemistry: Radical Sources, Spectra, Reaction Kinetics and Prediction Tools, 11, 3796-3822, https://doi.org/10.1002/cphc.201000533, 2010.
Herrmann, H., Schaefer, T., Tilgner, A., Styler, S. A., Weller, C., Teich, M., and Otto, T.: Tropospheric Aqueous-Phase Chemistry: Kinetics, Mechanisms, and Its Coupling to a Changing Gas Phase, Chem. Rev., 115, 4259-4334, http://dx.doi.org/10.1021/cr500447k, 2015.
Herrmann, H., Tilgner, A., Barzaghi, P., Majdik, Z., Gligorovski, S., Poulain, L., and Monod, A.: Towards a more detailed description of tropospheric aqueous phase organic chemistry: CAPRAM 3.0, 39, 4351-4363, https://doi.org/10.1016/j.atmosenv.2005.02.016, 2005.
Hoffmann, D., Weigert, B., Barzaghi, P., and Herrmann, H.: Reactivity of poly-alcohols towards OH, NO_3 and SO_4^- in aqueous solution, 11, 9351-9363, https://doi.org/10.1039/B908459B, 2009.
Hunter, J. F., Carrasquillo, A. J., Daumit, K. E., and Kroll, J. H.: Secondary Organic Aerosol Formation from Acyclic, Monocyclic, and Polycyclic Alkanes, 48, 10227-10234, https://doi.org/10.1021/es502674s, 2014.
Jimenez, J. L., Canagaratna, M. R., Donahue, N. M., Prevot, A. S. H., Zhang, Q., Kroll, J. H., DeCarlo, P. F., Allan, J. D., Coe, H., Ng, N. L., Aiken, A. C., Docherty, K. S., Ulbrich, I. M., Grieshop, A. P., Robinson, A. L., Duplissy, J., Smith, J. D., Wilson, K. R., Lanz, V. A., Hueglin, C., Sun, Y. L., Tian, J., Laaksonen, A., Raatikainen, T., Rautiainen, J., Vaattovaara, P., Ehn, M., Kulmala, M., Tomlinson, J. M., Collins, D. R., Cubison, M. J., Dunlea, J., Huffman, J. A., Onasch, T. B., Alfarra, M. R., Williams, P. I., Bower, K., Kondo, Y., Schneider, J., Drewnick, F., Borrmann, S., Weimer, S., Demerjian, K., Salcedo, D., Cottrell, L., Griffin, R., Takami, A., Miyoshi, T., Hatakeyama, S., Shimono, A., Sun, J. Y., Zhang, Y. M., Dzepina, K., Kimmel, J. R., Sueper, D., Jayne, J. T., Herndon, S. C., Trimborn, A. M.,

595 Williams, L. R., Wood, E. C., Middlebrook, A. M., Kolb, C. E., Baltensperger, U., and Worsnop, D. R.: Evolution of Organic Aerosols in the Atmosphere, 326, 1525-1529, 10.1126/science.1180353, 2009.
Klein, R. A.: Hydrogen bonding in diols and binary diol–water systems investigated using DFT methods. II. Calculated infrared OH-stretch frequencies, force constants, and NMR chemical shifts correlate with hydrogen bond geometry and electron density topology. A reevaluation of geometrical criteria for hydrogen bonding, 24,
600 1120-1131, https://doi.org/10.1002/jcc.10256, 2003.
Konjević, L., Racar, M., Ilinčić, P., and Faraguna, F.: A comprehensive study on application properties of diesel blends with propanol, butanol, isobutanol, pentanol, hexanol, octanol and dodecanol, 262, 125430, https://doi.org/10.1016/j.energy.2022.125430, 2023.
Kopinke, F.-D. and Georgi, A.: What Controls Selectivity of Hydroxyl Radicals in Aqueous Solution? Indications
605 for a Cage Effect, 121, 7947-7955, https://doi.org/10.1021/acs.jpca.7b05782, 2017.
Kroflič, A., Schaefer, T., Huš, M., Phuoc Le, H., Otto, T., and Herrmann, H.: OH radicals reactivity towards phenol-related pollutants in water: temperature dependence of the rate constants and novel insights into the [OH–phenol]˙ adduct formation, 22, 1324-1332, https://doi.org/10.1039/C9CP05533A, 2020.
Kwok, E. S. C. and Atkinson, R.: Estimation of hydroxyl radical reaction rate constants for gas-phase organic
610 compounds using a structure-reactivity relationship: An update, 29, 1685-1695, https://doi.org/10.1016/1352-2310(95)00069-B, 1995.
Leviss, D. H., Van Ry, D. A., and Hinrichs, R. Z.: Multiphase Ozonolysis of Aqueous α-Terpineol, 50, 11698-11705, https://doi.org/10.1021/acs.est.6b03612, 2016.
Lim, Y. B. and Ziemann, P. J.: Effects of Molecular Structure on Aerosol Yields from OH Radical-Initiated
615 Reactions of Linear, Branched, and Cyclic Alkanes in the Presence of NOx, 43, 2328-2334, https://doi.org/10.1021/es803389s, 2009.
Lin, G., Sillman, S., Penner, J. E., and Ito, A.: Global modeling of SOA: the use of different mechanisms for aqueous-phase formation, 14, 5451-5475, 10.5194/acp-14-5451-2014, 2014.
Luo, X., Yang, X., Qiao, X., Wang, Y., Chen, J., Wei, X., and Peijnenburg, W. J. G. M.: Development of a QSAR
620 model for predicting aqueous reaction rate constants of organic chemicals with hydroxyl radicals, 19, 350-356, https://doi.org/10.1039/c6em00707d, 2017.
Database for the Kinetics of the Gas-Phase Atmospheric Reactions of Organic Compounds, update May 10, 2021, last access: Last visit 20.08.2022.
Mahilang, M., Deb, M. K., and Pervez, S.: Biogenic secondary organic aerosols: A review on formation
625 mechanism, analytical challenges and environmental impacts, 262, 127771, https://doi.org/10.1016/j.chemosphere.2020.127771, 2021.
Matheson, M. S., Mamou, A., Silverman, J., and Rabani, J.: Reaction of hydroxyl radicals with polyethylene oxide in aqueous solution, 77, 2420-2424, https://doi.org/10.1021/j100639a011, 1973.
McGillen, Carter, W. P. L., Mellouki, A., Orlando, J. J., Picquet-Varrault, B., and Wallington, T. J.: Database for the
630 kinetics of the gas-phase atmospheric reactions of organic compounds, 12, 1203-1216, https://doi.org/10.5194/essd-12-1203-2020, 2020.
McGillen, W. P. L. Carter, A. Mellouki, J. J. Orlando, B. Picquet-Varrault, and Wallington, a. T. J.: Database for the Kinetics of the Gas-Phase Atmospheric Reactions of Organic Compounds, update May 10, 2021, 2022, https://doi.org/10.25326/mh4q-y215., 2021.
635 McNeill, V. F.: Aqueous Organic Chemistry in the Atmosphere: Sources and Chemical Processing of Organic Aerosols, 49, 1237-1244, https://doi.org/10.1021/es5043707, 2015.

https://doi.org/10.5194/egusphere-2023-1381
Preprint. Discussion started: 14 August 2023

McVay, R. and Ervens, B.: A microphysical parameterization of aqSOA and sulfate formation in clouds, 44, 7500-7509, 10.1002/2017gl074233, 2017.
Mekic, M. and Gligorovski, S.: Ionic strength effects on heterogeneous and multiphase chemistry: Clouds versus aerosol particles, 244, 117911, https://doi.org/10.1016/j.atmosenv.2020.117911, 2021.
Mellouki, A., Le Bras, G., and Sidebottom, H.: Kinetics and Mechanisms of the Oxidation of Oxygenated Organic Compounds in the Gas Phase, 103, 5077-5096, https://doi.org/10.1021/cr020526x, 2003.
Mellouki, A., Wallington, T. J., and Chen, J.: Atmospheric Chemistry of Oxygenated Volatile Organic Compounds: Impacts on Air Quality and Climate, 115, 3984-4014, https://doi.org/10.1021/cr500549n, 2015.
Minakata, D., Li, K., Westerhoff, P., and Crittenden, J.: Development of a Group Contribution Method To Predict Aqueous Phase Hydroxyl Radical (HO•) Reaction Rate Constants, 43, 6220-6227, https://doi.org/10.1021/es900956c, 2009.
Monod, A. and Doussin, J. F.: Structure-activity relationship for the estimation of OH-oxidation rate constants of aliphatic organic compounds in the aqueous phase: alkanes, alcohols, organic acids and bases, 42, 7611-7622, https://doi.org/10.1016/j.atmosenv.2008.06.005, 2008.
Murakami, M. and Ishida, N.: β-Scission of Alkoxy Radicals in Synthetic Transformations, 46, 1692-1700, https://doi.org/10.1246/cl.170834, 2017.
Otto, S. and Engberts, J. B. F. N.: Hydrophobic interactions and chemical reactivity, 1, 2809-2820, https://doi.org/10.1039/B305672D, 2003.
Otto, T., Schaefer, T., and Herrmann, H.: Aqueous-Phase Oxidation of Terpene-Derived Acids by Atmospherically Relevant Radicals, 122, 9233-9241, https://doi.org/10.1021/acs.jpca.8b08922, 2018.
Pai, S. J., Heald, C. L., Pierce, J. R., Farina, S. C., Marais, E. A., Jimenez, J. L., Campuzano-Jost, P., Nault, B. A., Middlebrook, A. M., Coe, H., Shilling, J. E., Bahreini, R., Dingle, J. H., and Vu, K.: An evaluation of global organic aerosol schemes using airborne observations, 20, 2637-2665, 10.5194/acp-20-2637-2020, 2020.
Park, H.-R. and Getoff, N.: Radiolysis of Aqueous Ethanol in the Presence of CO, 47, 985-991, https://doi.org/10.1515/zna-1992-0909, 1992.
Peduzzi, P., Concato, J., Kemper, E., Holford, T. R., and Feinstein, A. R.: A simulation study of the number of events per variable in logistic regression analysis, 49, 1373-1379, https://doi.org/10.1016/S0895-4356(96)00236-3, 1996.
Pye, H. O. T., Ward-Caviness, C. K., Murphy, B. N., Appel, K. W., and Seltzer, K. M.: Secondary organic aerosol association with cardiorespiratory disease mortality in the United States, 12, 7215, 10.1038/s41467-021-27484-1, 2021.
Rauk, A., Boyd, R. J., Boyd, S. L., Henry, D. J., and Radom, L.: Alkoxy radicals in the gaseous phase: β-scission reactions and formation by radical addition to carbonyl compounds, 81, 431-442, https://doi.org/10.1139/v02-206, 2003.
Reuvers, A. P., Greenstock, C. L., Borsa, J., and Chapman, J. D.: Studies on the Mechanism of Chemical Radioprotection by Dimethyl Sulphoxide, 24, 533-536, http://doi.org/10.1080/09553007314551431, 1973.
Richters, S., Herrmann, H., and Berndt, T.: Gas-phase rate coefficients of the reaction of ozone with four sesquiterpenes at 295 ± 2 K, 17, 11658-11669, https://doi.org/10.1039/C4CP05542J, 2015.
Russell, G. A.: Deuterium-isotope Effects in the Autoxidation of Aralkyl Hydrocarbons. Mechanism of the Interaction of PEroxy Radicals[1], 79, 3871-3877, https://doi.org/10.1021/ja01571a068, 1957.
Sander, R.: Compilation of Henry's law constants (version 4.0) for water as solvent, 15, 4399-4981, https://doi.org/10.5194/acp-15-4399-2015, 2015.

Sarang, K., Otto, T., Rudzinski, K., Schaefer, T., Grgić, I., Nestorowicz, K., Herrmann, H., and Szmigielski, R.: Reaction Kinetics of Green Leaf Volatiles with Sulfate, Hydroxyl, and Nitrate Radicals in Tropospheric Aqueous Phase, 55, 13666-13676, https://doi.org/10.1021/acs.est.1c03276, 2021.

Sato, K., Jia, T., Tanabe, K., Morino, Y., Kajii, Y., and Imamura, T.: Terpenylic acid and nine-carbon multifunctional compounds formed during the aging of β-pinene ozonolysis secondary organic aerosol, 130, 127-135, https://doi.org/10.1016/j.atmosenv.2015.08.047, 2016.

Schaefer, T., Wen, L., Estelmann, A., Maak, J., and Herrmann, H.: pH- and Temperature-Dependent Kinetics of the Oxidation Reactions of OH with Succinic and Pimelic Acid in Aqueous Solution, 11, 320, https://doi.org/10.3390/atmos11040320, 2020.

Scholes, G. and Willson, R. L.: γ-Radiolysis of aqueous thymine solutions. Determination of relative reaction rates of OH radicals, 63, 2983-2993, https://doi.org/10.1039/TF9676302983, 1967.

Schöne, L., Schindelka, J., Szeremeta, E., Schaefer, T., Hoffmann, D., Rudzinski, K. J., Szmigielski, R., and Herrmann, H.: Atmospheric aqueous phase radical chemistry of the isoprene oxidation products methacrolein, methyl vinyl ketone, methacrylic acid and acrylic acid – kinetics and product studies, 16, 6257-6272, https://doi.org/10.1039/C3CP54859G, 2014.

Shrivastava, M., Cappa, C. D., Fan, J., Goldstein, A. H., Guenther, A. B., Jimenez, J. L., Kuang, C., Laskin, A., Martin, S. T., Ng, N. L., Petaja, T., Pierce, J. R., Rasch, P. J., Roldin, P., Seinfeld, J. H., Shilling, J., Smith, J. N., Thornton, J. A., Volkamer, R., Wang, J., Worsnop, D. R., Zaveri, R. A., Zelenyuk, A., and Zhang, Q.: Recent advances in understanding secondary organic aerosol: Implications for global climate forcing, 55, 509-559, https://doi.org/10.1002/2016RG000540, 2017.

Sindelarova, K., Markova, J., Simpson, D., Huszar, P., Karlicky, J., Darras, S., and Granier, C.: High-resolution biogenic global emission inventory for the time period 2000–2019 for air quality modelling, 14, 251-270, 10.5194/essd-14-251-2022, 2022.

Sindelarova, K., Granier, C., Bouarar, I., Guenther, A., Tilmes, S., Stavrakou, T., Müller, J. F., Kuhn, U., Stefani, P., and Knorr, W.: Global data set of biogenic VOC emissions calculated by the MEGAN model over the last 30 years, 14, 9317-9341, https://doi.org/10.5194/acp-14-9317-2014, 2014.

Smith, I. W. M. and Ravishankara, A. R.: Role of Hydrogen-Bonded Intermediates in the Bimolecular Reactions of the Hydroxyl Radical, 106, 4798-4807, https://doi.org/10.1021/jp014234w, 2002.

Su, H., Cheng, Y., and Pöschl, U.: New Multiphase Chemical Processes Influencing Atmospheric Aerosols, Air Quality, and Climate in the Anthropocene, 53, 2034-2043, 10.1021/acs.accounts.0c00246, 2020.

Swain, C. G. and Lupton, E. C.: Field and resonance components of substituent effects, 90, 4328-4337, https://doi.org/10.1021/ja01018a024, 1968.

Tsigaridis, K. and Kanakidou, M.: The Present and Future of Secondary Organic Aerosol Direct Forcing on Climate, 4, 84-98, https://doi.org/10.1007/s40641-018-0092-3, 2018.

Tsui, W. G., Woo, J. L., and McNeill, V. F.: Impact of Aerosol-Cloud Cycling on Aqueous Secondary Organic Aerosol Formation, 10, 666, 2019.

von Sonntag, C. and Schuchmann, H.-P.: The Elucidation of Peroxyl Radical Reactions in Aqueous Solution with the Help of Radiation-Chemical Methods, 30, 1229-1253, https://doi.org/10.1002/anie.199112291, 1991.

Witkowski, B., Al-sharafi, M., and Gierczak, T.: Kinetics of Limonene Secondary Organic Aerosol Oxidation in the Aqueous Phase, 52, 11583-11590, https://doi.org/10.1021/acs.est.8b02516, 2018a.

Witkowski, B., Al-sharafi, M., and Gierczak, T.: Kinetics and products of the aqueous-phase oxidation of β-caryophyllonic acid by hydroxyl radicals, 213, 231-238, https://doi.org/10.1016/j.atmosenv.2019.06.016, 2019.

https://doi.org/10.5194/egusphere-2023-1381
Preprint. Discussion started: 14 August 2023

Witkowski, B., Jurdana, S., and Gierczak, T.: Limononic Acid Oxidation by Hydroxyl Radicals and Ozone in the Aqueous Phase, 52, 3402-3411, https://doi.org/10.1021/acs.est.7b04867, 2018b.
Witkowski, B., al-Sharafi, M., Błaziak, K., and Gierczak, T.: Aging of α-Pinene Secondary Organic Aerosol by Hydroxyl Radicals in the Aqueous Phase: Kinetics and Products, 57, 6040-6051, https://doi.org/10.1021/acs.est.2c07630, 2023.
Witkowski, B., Chi, J., Jain, P., Błaziak, K., and Gierczak, T.: Aqueous OH kinetics of saturated C6–C10 dicarboxylic acids under acidic and basic conditions between 283 and 318 K; new structure-activity relationship parameters, 267, 118761, https://doi.org/10.1016/j.atmosenv.2021.118761, 2021.
Xu, L., Du, L., Tsona, N. T., and Ge, M.: Anthropogenic Effects on Biogenic Secondary Organic Aerosol Formation, 38, 1053-1084, 10.1007/s00376-020-0284-3, 2021.
Yasmeen, F., Szmigielski, R., Vermeylen, R., Gómez-González, Y., Surratt, J. D., Chan, A. W. H., Seinfeld, J. H., Maenhaut, W., and Claeys, M.: Mass spectrometric characterization of isomeric terpenoic acids from the oxidation of α-pinene, β-pinene, d-limonene, and Δ3-carene in fine forest aerosol, 46, 425-442, https://doi.org/10.1002/jms.1911, 2011.
Zhao, R., Aljawhary, D., Lee, A. K. Y., and Abbatt, J. P. D.: Rapid Aqueous-Phase Photooxidation of Dimers in the α-Pinene Secondary Organic Aerosol, 4, 205-210, https://doi.org/10.1021/acs.estlett.7b00148, 2017.
Zhou, W., Mekic, M., Liu, J., Loisel, G., Jin, B., Vione, D., and Gligorovski, S.: Ionic strength effects on the photochemical degradation of acetosyringone in atmospheric deliquescent aerosol particles, 198, 83-88, https://doi.org/10.1016/j.atmosenv.2018.10.047, 2019.
Zhu, Y., Tilgner, A., Hoffmann, E. H., Herrmann, H., Kawamura, K., Yang, L., Xue, L., and Wang, W.: Multiphase MCM–CAPRAM modeling of the formation and processing of secondary aerosol constituents observed during the Mt. Tai summer campaign in 2014, 20, 6725-6747, https://doi.org/10.5194/acp-20-6725-2020, 2020.